THESIS FOR THE DEGREE OF DOCTOR OF PHILOSOPHY

# Towards Context Information-based High-Performing Connectivity in Internet of Vehicle Communications

HAO GUO

CHALMERS
UNIVERSITY OF TECHNOLOGY

Communication Systems Group
Department of Electrical Engineering
Chalmers University of Technology
Gothenburg, Sweden, 2022

**Towards Context Information-based High-Performing Connectivity in Internet of Vehicle Communications**

Hao Guo



ISBN: 978-91-7905-615-5
Doktorsavhandlingar vid Chalmers tekniska högskola
Ny serie 5081
ISSN 0346-718X

This thesis has been prepared using LaTeX.

Communication Systems Group
Department of Electrical Engineering
Chalmers University of Technology
SE-412 96 Gothenburg, Sweden
Phone: +46 (0)31 772 1000
www.chalmers.se

Printed by Chalmers Reproservice
Gothenburg, Sweden, January 2022

*To my parents*

“Take the sourest lemon life has to offer you and turn it into something resembling lemonade.”

*–This Is Us*

# Abstract

Internet-of-vehicles (IoV) is one of the most important use cases in the fifth generation (5G) of wireless networks and beyond. Here, IoV communications refer to two types of scenarios: serving the in-vehicle users with moving relays (MRs); and supporting vehicle-to-everything (V2X) communications for, e.g., connected vehicle functionalities. Both of them can be achieved by transceivers on top of vehicles with growing demand for quality of service (QoS), such as spectrum efficiency, peak data rate, and coverage probability. However, the performance of MRs and V2X is limited by challenges such as the inaccurate prediction/estimation of the channel state information (CSI), beamforming mismatch, and blockages. Knowing the environment and utilizing such context information to assist communication could alleviate these issues. This thesis investigates various context information-based performance enhancement schemes for IoV networks, with main contributions listed as follows.

In order to mitigate the channel aging issue, i.e., the CSI becomes inaccurate soon at high speeds, the first part of the thesis focuses on one way to increase the prediction horizon of CSI in MRs: predictor antennas (PAs). A PA system is designed as a system with two sets of antennas on the roof of a vehicle, where the PAs positioned at the front of the vehicle are used to predict the CSI observed by the receive antennas (RAs) that are aligned behind the PAs. In PA systems, however, the benefit is affected by a variety of factors. For example, 1) spatial mismatch between the point where the PA estimates the channel and the point where the RA reaches several time slots later, 2) antenna utilization efficiency of the PA, 3) temporal evolution, and 4) estimation error of the PA-base station (BS) channel.

First, in Paper A, we study the PA system in the presence of the spatial mismatch problem, and propose an analytical channel model which is used for rate adaptation. In paper B, we propose different approximation schemes for the analytical investigation of PA systems, and study the effect of different parameters on the network performance. Then, involving PAs into data transmission, Paper C and Paper D analyze the outage- and the delay-limited performance of PA systems using hybrid automatic repeat request (HARQ), respectively. As we show in the analytical and the simulation results in Papers C-D, the combination of PA and HARQ protocols makes it possible to improve spectral efficiency and adapt the transmission parameters to mitigate the effect of spatial mismatch. Finally, a review of PA studies in the literature, the challenges and potentials of PA as well as some to-be-solved issues are presented in Paper E.

The second part of the thesis focuses on using advanced technologies to further improve the MR/IoV performance. In Paper F, a cooperative PA scheme in IoV networks is proposed to mitigate both the channel aging effect and blockage sensitivity in millimeter-wave channels by collaborative vehicles and BS handover. Then, in Paper G, we study the potentials and challenges of dynamic blockage pre-avoidance

in IoV networks.

**Keywords:** 5G/B5G, 6G, blockage, channel state information (CSI), integrated access and backhaul (IAB), Internet-of-vehicles (IoV), Marcum Q-function, millimeter wave, mobile relay, outage probability, predictor antenna, rate adaptation, reconfigurable intelligent surface, relay, spatial correlation, temporal correlation, throughput, vehicle-to-everything (V2X), wireless backhaul.

# List of Publications

This thesis is based on the following publications:

[A] **H. Guo**, B. Makki, and T. Svensson, "Rate adaptation in predictor antenna systems," *IEEE Wireless Communications Letters*, vol. 9, no. 4, pp. 448-451, Apr. 2020.

[B] **H. Guo**, B. Makki, M.-S. Alouini, and T. Svensson, "A semi-linear approximation of the first-order Marcum $Q$-function with application to predictor antenna systems," *IEEE Open Journal of Communication Society*, vol. 2, pp. 273-286, Feb. 2021.

[C] **H. Guo**, B. Makki, M.-S. Alouini, and T. Svensson, "Power allocation in HARQ-based predictor antenna systems," *IEEE Wireless Communication Letters*, vol. 9, no. 12, pp. 2025-2029, Dec. 2020.

[D] **H. Guo**, B. Makki, M.-S. Alouini, and T. Svensson, "On the delay-limited average rate of HARQ-based predictor antenna systems," *IEEE Wireless Communication Letters*, vol. 10, no. 8, pp. 1628-1632, Aug. 2021.

[E] **H. Guo**, B. Makki, D.-T. Phan-Huy, E. Dahlman, M.-S. Alouini, T. Svensson, "Predictor antenna: A technique to boost the performance of moving relays," *IEEE Communications Magazine*, vol. 59, no. 7, pp. 80-86, Jul. 2021.

[F] **H. Guo**, B. Makki, M.-S. Alouini, and T. Svensson, "High-rate uninterrupted internet-of-vehicle communications in highways: Dynamic blockage avoidance and CSIT acquisition," *IEEE Communications Magazine*, major revision, Jan. 2022.

[G] **H. Guo**, B. Makki, M. Åström, M.-S. Alouini, and T. Svensson, "Dynamic blockage pre-avoidance using reconfigurable intelligent surfaces," submitted to *IEEE Communications Magazine*, Jan. 2022.

Other publications by the author, not included in this thesis, are:

[H] **H. Guo**, B. Makki, and T. Svensson, "Velocity-aware antenna selection in predictor antenna systems," invited paper in *Proc. IEEE WSA*, French Riviera, Nov. 2021, pp. 1-5.

[I] **H. Guo**, B. Makki, and T. Svensson, "Predictor antennas for moving relays: Finite block-length analysis," invited paper in *Proc. IEEE CommNet*, Marrakech, Morocco, Sept. 2020, pp. 1-8.

[J] **H. Guo**, B. Makki, and T. Svensson, "A genetic algorithm-based beamforming approach for delay-constrained networks," in *Proc. IEEE WiOpt*, Paris, France, May 2017, pp. 1-7.

[K] **H. Guo**, B. Makki, and T. Svensson, "A comparison of beam refinement algorithms for millimeter wave initial access," in *Proc. IEEE PIMRCW*, Montreal, QC, Canada, Oct. 2017, pp. 1-7.

[L] **H. Guo**, B. Makki, and T. Svensson, "Genetic algorithm-based beam refinement for initial access in millimeter wave mobile networks," *Wireless Communication and Mobile Computing*, Jun. 2018.

## Acknowledgments

First and foremost, I would like to express my deepest gratitude to Prof. Tommy Svensson for being my examiner and main supervisor, for allowing me to become a full-year master thesis student and later a Ph.D. candidate, and for helping me learn to be an independent researcher and overall a more interesting person. It has been such a wonderful journey with you since we first met in Nankai seven years ago, and thank you for your constant supports over the years.

My deepest gratitude also goes to my co-supervisor, Dr. Behrooz Makki, for thousands of emails from you, containing your brilliant ideas and valuable comments, for the fruitful meetings whenever I need them, and for various opportunities you have been offering me, such as journal reviews and research collaborations. I recommend everyone to collaborate with you and enjoy your kind, friendly, and pure personality.

I would like to send my gratitude to some distinguished researchers who have mentored me over the years. Thank you, Prof. Mohamed-Slim Alouini, Dr. Phan-Huy Dinh-Thuy, Dr. Erik Dahlman, and Dr. Magnus Åström for contributing to our work with wonderful ideas and different perspectives. Thank you, Dr. Jingya Li, Dr. Jinlin Liu, Prof. Jun Li, and Dr. Kai Guo for being role models for me, and for all the insights you have given me beyond my research. I am also grateful to Prof. Mikael Sternad, Prof. Carmen Botella, Prof. Xiaoming Chen, Prof. Fuxi Wen, and Dr. Nima Jamaly for all the nice discussions and collaborations we have had. I would also like to thank my opponent Prof. Eduard Jorswieck and committee members Prof. Zhu Han, Prof. Marina Petrova, and Dr. Fredrik Harrysson for agreeing on attending my defense, and the valuable time for pre-evaluation and discussions.

I would like to thank all the current and former members of the Communication Systems group. Many thanks to the head of our division, Prof. Erik Ström, and the head of our group, Prof. Fredrik Brännström, for ensuring a stimulating and joyful research atmosphere. Special thanks to Prof. Erik Agrell for our nice collaborations in our teaching work, and for everything you have shown me to be a kind and responsible teacher. Also, many thanks go to Professors Giuseppe Durisi, Henk Wymeersch, Alexandre Graell i Amat, Thomas Eriksson, Christian Häger, and Jian Yang for very interesting discussions in the courses. Gratitude also goes to Agneta, Natasha, Daniela, Annie, Anna, Yvonne, and Madeleine for all your supports. Last but not least, I am glad to be one part of the Wireless Systems team, and thank you all for the great efforts to contribute to such a wonderful research area.

Thank you, Chao, Chenjie, Xinlin, Lei, Yuxuan, Dapeng, Sven, Rahul, Johan, Keerthi, and Anver for being my big brothers and helping me through the early stages of my doctoral study. On the other end, many thanks to Roman, Shen, Chouaib, and Hyowon for the proofreading of my thesis and of course, you make my life better from much more angles. Thank you, Li, Cristian, Björn, and Lise for your amazing work in our teaching course. I would also like to thank all my Chinese friends in Gothenburg for all the great moments we have experienced together.

Special thanks go to Xiao, Chi, Yu, Yibo, Mengqiao, Mengcheng, Pei, and Qiang for always being there for me.

Thank you Hongxu, for always showing me the right direction at the right moment.

Thank you Yigeng, for all the support and encouragement you have given to me.

Finally, I would like to express my sincerest gratitude to my family. Thank you my great-grandmother for your strong belief in me. Thank you my cousin Bao for your support and encouragement. Thank you Chouchou for coming into my life and instantly becoming an absolute delight.

Mom and dad: Thank you for giving me life and teaching me how to add meaning to it. My life would have been totally different without your dedication and love. A "Thank you" is far from enough for you! I love you.

Hao Guo
Göteborg, January 2022

# Financial Support

This work was supported in part by VINNOVA (Swedish Government Agency for Innovation Systems) within the project "Smart wireless networking for green ICT" and the VINN Excellence Center ChaseOn, and in part by the EC within the H2020 projects mmMAGIC and 5GCAR. The simulations were performed in part on resources provided by the Swedish National Infrastructure for Computing (SNIC) at C3SE.

# Acronyms

| | |
|---|---|
| **2G/4G/5G/B5G** | Second/Fourth/Fifth/Beyond Fifth generation |
| **3GPP** | 3rd generation partnership project |
| **ACK** | Acknowledgment |
| **ARQ/HARQ** | Automatic repeat request/Hybrid automatic repeat request |
| **BF** | Beamforming |
| **CDF** | Cumulative distribution function |
| **CSI** | Channel state information |
| **CSIT** | Channel state information at the transmitter |
| **DL** | Downlink |
| **DFT** | Discrete Fourier Transform |
| **EMBB** | Enhanced mobile broadband |
| **E2E** | End-to-end |
| **FDD** | Frequency division duplex |
| **FSO** | Free-space optical |
| **GPS** | Global positioning system |
| **IAB** | Integrated access and backhaul |
| **i.i.d.** | Identical and independently distributed |
| **INR** | Incremental redundancy |
| **IoV** | Internet-of-vehicles |
| **LoS** | Line-of-sight |
| **LSCPA** | Large-scale cooperative PA |
| **LSRPA** | Large-scale based RIS pre-assignment |
| **LTE** | Long-term evolution |
| **MIMO** | Multiple-input multiple-output |

| | |
|---|---|
| **MISO** | Multiple-input single-output |
| **mmw** | Millimeter wave |
| **MR** | Moving relay |
| **MRN** | Moving relay node |
| **MRT** | Maximum ratio transmission |
| **MTC** | Machine-type communications |
| **NACK** | Negative acknowledgment |
| **NLoS** | Non-line-of-sight |
| **NMSE** | Normalized mean squared error |
| **npcu** | Nats-per-channel-use |
| **NR** | New Radio |
| **OFDM** | Orthogonal frequency-division multiplexing |
| **PA** | Predictor antenna |
| **PDF** | Probability density function |
| **QoS** | Quality of service |
| **RA** | Receive antenna |
| **RF** | Radio-frequency |
| **RIS** | Reconfigurable intelligent surface |
| **RTD** | Repetition time diversity |
| **SNR** | Signal-to-noise ratio |
| **SINR** | Signal-to-interference-plus-noise ratio |
| **TDD** | Time division duplex |
| **UL** | Uplink |
| **URLLC** | Ultra-reliable low-latency communications |
| **V2X** | Vehicle-to-everything |
| **ZF** | Zero-forcing |

# Contents

**Abstract** i

**List of Papers** iii

**Acknowledgements** v

**Acronyms** ix

**I Overview 1**

**1 Introduction 3**

1.1 Background . . . . . . . . . . . . . . . . . . . . . . . . . . 3
1.1.1 Internet of Vehicles in 5G/B5G . . . . . . . . . . . . . . . . . . 4
1.1.2 Channel Characteristics in Vehicle Communications . . . . . . 5
1.1.3 Predictor Antenna: A Possible CSIT Acquisition Technique at High Speeds . . . . . . . . . . . . . . . . . . . . . . . . . . 7
1.1.4 Potential of Reconfigurable Intelligent Surface . . . . . . . . . . 8
1.2 Scope of the Thesis . . . . . . . . . . . . . . . . . . . . . . . . 9
1.3 Organization of the Thesis . . . . . . . . . . . . . . . . . . . . 10

**2 Predictor Antenna Systems and Channel Model 11**

2.1 Overview of Predictor Antenna Setup . . . . . . . . . . . . . . . . . 11
2.2 PA Validation by Testbed-based Experimental Evaluations . . . . . . 13
2.2.1 The First Experiment of the PA . . . . . . . . . . . . . . . . . 13
2.2.2 Test in Dresden, Germany in 2014 . . . . . . . . . . . . . . . . 14
2.2.3 Test in Dresden, Germany in 2017 . . . . . . . . . . . . . . . . 14

2.2.4 Test in Stuttgart, Germany in 2018 . . . . . . . . . . . . . . . . 15
2.3 Challenges and Difficulties . . . . . . . . . . . . . . . . . . . . . . . . 15
2.4 Proposed Analytical Channel Model . . . . . . . . . . . . . . . . . . . . 17
2.5 First-Order Marcum Q-Function and Semi-Linear Approximation . . . 19

**3 Performance Enhancement Using Resource Allocation in PA Systems 23**
3.1 Rate Adaptation in the Classic PA Setup . . . . . . . . . . . . . . . . 23
3.2 Hybrid Automatic Repeat Request in the PA Systems . . . . . . . . . 24
3.3 Outage-constrained Power Allocation in the HARQ-based PA Systems 26
3.4 Delay-limited Average Rate Optimization in the HARQ-based PA Systems . . . . . . . . . . . . . . . . . . . . . . . . . . . . . . . . 29
3.5 Adaptive Delay Transmission . . . . . . . . . . . . . . . . . . . . . . . 31

**4 Towards Practical MRs: Cooperative Systems at MmWave 33**
4.1 Massive MIMO Beamforming-based PA Systems . . . . . . . . . . . . 33
4.2 Dynamic Blockage Avoidance . . . . . . . . . . . . . . . . . . . . . . . 35
4.2.1 Background: Encounter Blockage at mmW . . . . . . . . . . . 35
4.2.2 Existing Methodologies . . . . . . . . . . . . . . . . . . . . . . 36
4.2.3 Proposed Scheme with Cooperative PA . . . . . . . . . . . . . 36
4.2.4 Dynamic Blockage Pre-Avoidance Using RIS . . . . . . . . . . 39

**5 Contributions and Future Work 43**
5.1 Paper A . . . . . . . . . . . . . . . . . . . . . . . . . . . . . . . . . 44
5.2 Paper B . . . . . . . . . . . . . . . . . . . . . . . . . . . . . . . . . 45
5.3 Paper C . . . . . . . . . . . . . . . . . . . . . . . . . . . . . . . . . 45
5.4 Paper D . . . . . . . . . . . . . . . . . . . . . . . . . . . . . . . . . 45
5.5 Paper E . . . . . . . . . . . . . . . . . . . . . . . . . . . . . . . . . 46
5.6 Paper F . . . . . . . . . . . . . . . . . . . . . . . . . . . . . . . . . 46
5.7 Paper G . . . . . . . . . . . . . . . . . . . . . . . . . . . . . . . . . 47
5.8 Related Contributions . . . . . . . . . . . . . . . . . . . . . . . . . . 47
5.9 Future work . . . . . . . . . . . . . . . . . . . . . . . . . . . . . . . 48

**References 51**

**II Papers 63**

# Part I

# Overview

# CHAPTER 1

# Introduction

## 1.1 Background

Nowadays, wireless communications and their related applications play an important role in our life. Since the first mobile communication system was employed in the early 1980s, new standards were established roughly every ten years, leading to the first commercial deployments of the fifth generation (5G) cellular networks in late 2019 [1]–[3]. Modern wireless technologies have been developing from the second generation (2G) where the first digital communication system was deployed with text messages being available, through the recent fourth generation (4G) with Long-Term Evolution (LTE) being the dominant technology, which supports much higher data rate with lower latency, towards future beyond 5G (B5G) with New Radio (NR) standardized by the 3rd generation partnership project (3GPP) [4]. Among these exciting achievements, one theme never changes: the growing demand for high-speed, ultra-reliable, low-latency, and energy-efficient wireless communications with limited radio spectrum resource.

According to the Ericsson mobility report in June 2021, the total number of mobile subscriptions has exceeded 8 billion today, with 4G being the major standard, and it is expected that this number will reach around 8.8 billion with over 30% being supported by NR by the end of 2026 [1]. Thanks to the higher bandwidth at millimeter wave frequency spectrum as well as the development of multi-antenna techniques, new use cases in 5G, such as intelligent transport systems, autonomous vehicle control, virtual reality, factory automation, and providing coverage to high-mobility users, have been developed rapidly [5]. These use cases are usually categorized into three distinct classes by the standardization groups of 5G [6]:

i) Enhanced mobile broadband (EMBB) deals with large data packets and how to deliver them using high data rates [7]. This can be seen as a natural extension of the current established LTE system that is designed for the similar use case. Typical EMBB applications involve high-definition video streaming, virtual reality, and online gaming.

ii) Massive machine-type communications (MTC) is a new application in 5G, which targets at providing wide coverage to a massive number of devices such as sensors which send sporadic updates to a base station (BS) [8]. Here, the key requirements are energy consumption, reliability, and scalability. High data rate and low latency, on the other hand, are of secondary importance.

iii) Ultra-reliable low-latency communications (URLLC) concerns applications with stringent requirements on reliability and latency [8]. In this type of use case, the challenge is to design protocols which can transmit data with very low error probability and fulfill the latency constraint at the same time. Applications falling into this category include real-time control in smart factories, remote medical surgery, and Internet-of-vehicles (IoV) communications which mainly focus on safety with high-mobility users.

This thesis targets both EMBB and URLLC. More specifically, we concentrate on efficient (high data rate) and reliable (low error/outage probability) IoV schemes with latency requirement, using technical enablers such as predictor antenna (PA) to obtain context information. The detailed review of IoV communications and the PA concept, as well as the associated research challenges, are presented in the following sub-sections.

### 1.1.1 Internet of Vehicles in 5G/B5G

Providing efficient, reliable broadband wireless communication links in high mobility use cases, such as high-speed railway systems and urban/highway vehicular communications, has been incorporated as an important part of 5G developments [9]. According to [10], 5G systems are expected to support a large number of users traveling at speeds up to 500 km/h, at a data rate of 150 Mbps or higher.

IoV refers to two different types of vehicle communications: 1) serving in-vehicle users and 2) supporting the connected-vehicle functionalities, and both of them can be well provided by the transceivers installed on top of vehicles. More specifically, the first scenario is normally referred to as moving relay (MR) or moving relay node (MRN), where a significant number of users could access cellular networks via MRs installed on top of, e.g., public transportation, such as buses, trams, and trains [11]. The main purpose of deploying MRs is to mitigate the impact of involving the vehicle into the propagation channel [12]. For example, the so-called vehicular penetration loss can be as high as 25 dB in a minivan at the frequency of 2.4 GHz [11]. As one type of MRN, one can consider the possible future deployment of integrated access and backhaul (IAB) nodes on top of the vehicles [13]–[15], where part of the radio resources is used for wireless backhauling. The second IoV functionality normally refers to as vehicle-to-everything (V2X), where the vehicle could communicate to, e.g., infrastructure (V2I), pedestrians (V2P), and other vehicles (V2V).

However, these dual functionalities of on-vehicle transceivers imply strict rate and reliability requirements, for which one may need to utilize large bandwidths, beamforming (BF), acquire up-to-date channel properties of a communication link (channel state information (CSI)), and avoid blockages, i.e., blocking of signals at high carrier frequencies such as millimeter wave (mmw).

Most current cellular systems can support users with low or moderate mobility, while high moving speed would limit coverage area and data rate significantly. For example, 4G systems are aimed at supporting users perfectly at the speed of 0-15 km/h, serving with high performance from 15 km/h to 120 km/h, and providing functional services at 120-350 km/h [16]. On the other hand, some field tests have shown that current 4G systems may only provide 2-4 Mbps data rate in high-speed trains [17]. To meet the requirement of high data rate at high moving speed in future mobility communication systems, new technologies that are able to cope with the challenges of mobility need to be developed.

Different techniques can be applied to improve the quality-of-service (QoS) at high speeds. For example, strategies in the current standard aiming at improving the spectral efficiency include multiple-input multiple-output (MIMO), CSI-based scheduling, and adaptive modulation and coding. Moreover, in future standardizations, techniques such as mmw, coordinated multipoint (CoMP) joint transmission (JT) [18], and massive MIMO may be also involved. All these enhancement techniques have one thing in common: They require accurate sensing/estimation of the environment with acceptable cost, among which channel state information at the transmitter (CSIT) is one of the major context information. However, it is not an easy task due to the characteristics of IoV channels in 5G/B5G.

### 1.1.2 Channel Characteristics in Vehicle Communications

Several features of IoV channels in 5G/B5G make it difficult to acquire CSIT [17]:

i) *Fast time-varying fading*: For high-speed vehicles, the channel has fast time-variation due to large Doppler spread. Let us consider a simple example. Assume a train operating at a speed of 200 km/h and a frequency of 6 GHz. Then, the maximum Doppler frequency is obtained by $f_{\mathrm{D}} = v/\lambda$ =1111 Hz, which corresponds to a channel coherence time of around 900 $\mu$s. However, in LTE the control loop time with both uplink (UL) and downlink (DL) is around

2 ms, which makes CSIT outdated if we consider time division duplex (TDD) system with channel reciprocity. Moreover, the speeds of moving terminals are usually time-varying, making the channel even more dynamic.

ii) *Channel estimation errors*: Due to the time-varying channel, it is not practical to assume perfect CSIT, as what we do for low-mobility systems. In fact, mobility makes it harder not only for accurately estimating the channel, but also for tracking, updating, and predicting the fading parameters. Also, the estimation error may have remarkable effects on system performance, which makes this aspect very important in system design.

iii) *Doppler diversity*: Doppler diversity has been developed for systems with perfect CSI, in which it provides diversity gain to improve system performance. On the other hand, Doppler diversity may cause high channel estimation errors, which makes it important to study the trade-off between Doppler diversity and estimation errors.

iv) *Lack of network planning*: With static networks, a large part of interference management and blockage avoidance is solved during the network planning. This may not be possible in high speeds with, e.g., unplanned interference and dynamic blockage.

Besides these aspects, there are also some issues for the channel with mobility, e.g., carrier frequency offset, inter-carrier interference, high penetration loss, and frequent handover. One important aspect is the blockage sensitivity of mmw. Moving towards mmw leads to more sufficient radio resources and the potential of multi-antenna techniques. However, the physical features of mmw signals could have strong impact on their applications: Besides the sensitivity to atmospheric variations, mmw propagation has high line-of-sight (LoS) path loss due to the reduced aperture that scales quadratically with the wavelength for a given number of antennas, and the signal quality could be significantly deteriorated by blockage.

With the existing methods and depending on the vehicle speed, channel coefficients may be outdated at the time of transmission, due to various delays in the control loop and the mobility of the vehicles. Also, when blockage occurs, lack of proper handling mechanism may lead to poor QoS at the receiver side.

The use of channel predictions can alleviate the outdated CSIT problem. By using the statistics over time and frequency, combined with linear predictors such as Kalman predictor, the channel coefficients can be predicted for around 0.1-0.3 carrier wavelengths in space [19]. This prediction horizon is enough for 4G systems with short control loops (1-2 ms) or for users with pedestrian velocities. On the other hand, the blockage issue could potentially be handled by resource association, cooperative transmission or the incorporation of relays. Back-up non-line-of-sight (NLoS) links could also be an option with proper selection of the NLoS path and

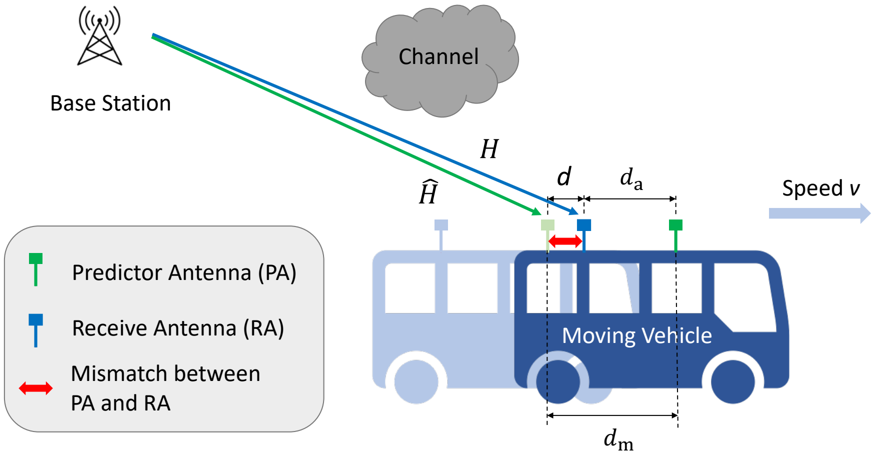


**Figure 1.1:** The PA concept with spatial mismatch problem.

potentially, additional deployment of reflectors. However, all of these methods are facing challenges and need to be refined for vehicular velocities at high frequencies.

### 1.1.3 Predictor Antenna: A Possible CSIT Acquisition Technique at High Speeds

To predict the channel in MRs, the concept of PA is proposed in [19]. Here, as shown in Fig. 1.1, PA system refers to a setup with two sets of antennas on the roof of a vehicle, where the PAs positioned in the front of the vehicle are used to predict the channel state observed by one receive antenna (RA) or a set of RAs that are aligned behind the PAs, and send the CSI back to the BS. Then, if the RA reaches the same point as the PA, the BS can use the CSI obtained from the PAs to improve the transmission to the RAs using, for example, power/rate adaptations and BF. The results in [19] indicate that the PA system can provide sufficiently accurate channel estimation for up to one wavelength in the LoS case.

Following [19], experimental validations are provided in [20]–[22] to prove the feasibility of the PA concept. Specifically, an order of magnitude increase of prediction horizons is presented in [20] compared to time-series-based prediction. Moreover, results in [21] show that the PA concept works for massive MIMO DLs where the PA can improve the signal-to-interference ratio in setups with NLoS channels. Also, authors in [22] demonstrate that the Kalman smoothing-based PA system enables 0.75 carrier wavelengths prediction at vehicle speeds for Rayleigh-like NLoS fading channels. The review of [19]–[22] reveals the following research problems:

i) *Speed sensitivity*: From the results in [20]–[22], we can observe that, for a given control loop time, if the speed is too high which leads to a spatial mismatch, i.e., the spot where the PA estimates the channel does not match the spot where the RA reaches at the second time slot, the accuracy of prediction decreases drastically. We can not make sure that the speed of the vehicle remains the same all the time, which may lead to performance loss. With a low speed, one can assume the PA could sample the space densely and store the CSI, and channel interpolation could potentially mitigate the mismatch. Moreover, studies in [23] and [24] have addressed this kind of spatial mismatch problem in the PA system to some extent. In [23], an interpolation-based BF scheme is proposed for DL multiple-input single-output (MISO) systems to solve the mis-pointing problem. From another perspective, results in [24] show the effect of velocity variation on prediction performance. However, how to analytically study speed sensitivity of the PA system remains unclear.

ii) *Lack of analytical model*: As we can see, the work in [19]–[22] are based on real-world testing data which validates the concept, while the study in [23] is based on simulated channel, and authors in [24] focus more on the antenna pattern. No analytical model of the PA system has been proposed in [19]–[24].

iii) *Performance enhancement the PA system*: As we can see from the results in [19]–[24], although the PA system can provide larger prediction horizons for up to three wavelengths, there is still a limit on the region, and the system is quite sensitive to vehicle speed. Hence, additional structure/schemes could potentially be built on top of the PA system to achieve better performance.

iv) *Application Scenarios of the PA system*: The key point of the PA concept is to use an additional antenna to acquire better quality of CSIT. In this way, the time-frequency resources of the PA are used for channel prediction instead of data transmission. Intuitively, there should exist a condition under which the PA concept could be helpful, compared to the case with simply using the PA as one of the RAs. Here, proper designs of the system may help us make such decisions. Moreover, with cooperative vehicle communication links and multi-BS handover, there is a potential to utilize the information provided by PAs on different vehicles to avoid not only the CSIT out-dating but also dynamic blockages in the following vehicles.

### 1.1.4 Potential of Reconfigurable Intelligent Surface

Besides deploying additional access points/BSs, reconfigurable intelligent surface (RIS) has recently emerged as an alternative solution to mitigate the blockage effect by manipulating the propagation environment [25]. With massive reflecting elements, RIS is capable of adjusting the direction of incoming radio waves to the desired directions. Compared to additional deployment of BSs, RIS requires no or low-cost dedicated power sources or radio-frequency (RF) chains. Also, it can be located with high flexibility and easily combined with various techniques, such as unmanned aerial vehicles with dual connectivity [26] and hybrid BF [27].

RIS is mainly used as a complement to the existing mobile network, and could improve the coverage of blind spots with LoS links. This is of particular interest in mmw frequencies due to the blockage sensitivity of mmw signals.

Despite the promising features of the RIS, there are several research challenges that require attention. Examples include imperfect transceivers, phase errors, and deployment optimizations. One of the major issues of the RIS-based system is that both the BS and the RIS require accurate CSIT in order to realise desired beam directions. If RF chains are deployed, one can switch the RIS into the absorbing mode and evaluate the known pilot symbols in order to estimate the channel. Also, the beams can be optimized without explicit CSIT. For example, one can use codebook-based BF and adjust the beam patterns by the feedback from the users. Statistical CSI could also be used for network optimizations [28]. However, these methods either require additional hardware, or the overhead of signal processing can be unacceptable. The problem becomes more challenging when it comes to IoV networks with rapidly changing channels and dynamic blockages. Deploying multiple RISs with proper path selection schemes could potentially alleviate the performance loss, but there is always a need for more efficient options.

## 1.2 Scope of the Thesis

The aim of this thesis is to investigate performance enhancement schemes using context information in IoV systems, with a focus on MR features. Starting from the CSIT acquisition for the MR, the PA concept as a promising solution is introduced. Based on simulation- and testbed-based studies in the literature, the spatial mismatch problem is highlighted followed by novel analytical channel models for the PA system. Then, different resource allocation schemes are proposed, e.g., rate adaptation, hybrid automatic repeat request (HARQ), outage-constrained power allocation, delay-limited average rate optimization, and adaptive delay transmission, to enhance the performance of the MR by exploiting the potential of knowing the CSIT. Then, with development of 5G/B5G, potential of practically deploy MRs are studied. Specifically, different MIMO schemes are investigated with the mismatch issue, and cooperative PA and RIS-based systems are designed for the dynamic blockage pre-avoidance.

The specific objectives of this thesis can be summarized as follows.

i) To characterize the speed sensitivity of the PA system by analytically modeling the channel in PA systems. (Chapter 2)

ii) To develop a mathematical tool in order to simplify the performance evaluation of the PA setup. (Chapter 2)

iii) To design efficient and reliable resource allocation schemes which are able to improve the performance of existing PA systems. (Chapter 3)

iv) To investigate the practical benefit of PA by comparing it with the state-of-the-art schemes under different scenarios. (Chapters 3-4)

v) To explore the potentials of IoV systems at mmw frequencies by utilizing cooperative vehicles and RIS-assisted setups to mitigate dynamic blockages. (Chapter 4)

## 1.3 Organization of the Thesis

Chapter 2 introduces and reviews the recent progress on the PA setups. Then, the spatial mismatch problem in the PA system is modeled using the so-called Marcum Q-function defined in, e.g., [29]. To help the analytical evaluations, a semi-linear approximation of the Marcum Q-function, with its applications on integral calculations and optimizations, is proposed.

Chapter 3 presents different resource allocation schemes to improve the performance of the PA system with the spatial mismatch problem. For each scheme, the problem formulation, the data transmission model, as well as the details of the proposed method are introduced.

Then, in Chapter 4, IoV networks are combined with recently emerged technologies and the potential of efficient and reliable MRs are revealed.

Finally, Chapter 5 provides a brief overview of the contributions in the appended papers, and discusses possible future research directions.

# CHAPTER 2

## Predictor Antenna Systems and Channel Model

This chapter first introduces the PA concept in a TDD DL system, where one PA and one RA are deployed at the receiver side. Also, the associated challenges of the PA systems are discussed. Then, the proposed analytical channel model based on Jake's assumption is presented, where the cumulative distribution function (CDF) of the channel gain is described by the first-order Marcum $Q$-function. Finally, to simplify the analytical derivations, we develop a semi-linear approximation of the first-order Marcum $Q$-function which can simplify, e.g., integral calculations as well as optimization problems.

## 2.1 Overview of Predictor Antenna Setup

In 5G, a significant number of users would access wireless networks in vehicles, e.g., in public transportation like trams and trains or in private cars, via their smart phones and laptops [11], [30]–[38]. In [30], the emergence of vehicular heavy user traffic is observed by field experiments conducted in 2012 and 2015 in Seoul, and the experimental results reveal that such traffic is becoming dominant, as shown by the 8.62 times increase from 2012 to 2015 in vehicular heavy user traffic, while in the same period the total traffic increased only 3.04 times. Setting an MRN in vehicles can be one promising solution to provide a high-rate reliable connection between a BS and the users inside the vehicle [11], [35], [36]. From another perspective, studies in [37] and [38] adopt femtocell technology inside a vehicle to provide better spectral and energy efficiency compared to the direct transmission scheme.

In such so-called hot spot scenario, we often deploy TDD systems with channel reciprocity because we typically consume more data in DL than UL. Here, we estimate the DL channel based on the UL pilots. Then, the problem may occur because of the movement, and the channel in the DL would not be the same as the one in the UL. This could be compensated for by extrapolating the CSI from the UL, for example by using Kalman predictions [39]. However, it is difficult to predict small-scale fading by extrapolating the past estimates, and the prediction horizon is limited to 0.1-0.3$\lambda$ with $\lambda$ being the carrier wavelength [40]. Such horizon is satisfactory for pedestrian users, while for high-mobility users, such as vehicles, a prediction horizon beyond 0.3$\lambda$ is usually required [22]. One possible way to increase the prediction horizon is to have a database of pre-recorded coordinate-specific CSI at the BSs [41]. Here, the basic idea is that the users provide the BSs with their location information by, e.g., global positioning system (GPS), and the BS could use the pre-recorded information to predict the channel environment. However, such method requires large amount of data, and the data may need to be updated frequently. In addition, the accuracy of location information is typically not sufficient to track small-scale fading.

To overcome this issue, the concept of PA is proposed in [19] wherein at least two antennas are deployed on top of the vehicle to enable online tracking of the small-scale fading. As can be seen in Fig. 1.1, the first antenna, which is the PA, estimates the channel $\hat{H}$ and sends feedback to the BS. Then, the BS uses the information received about $\hat{H}$ to estimate the channel $H$, and communicate with a second antenna, which we refer to as the RA, when it arrives to the same position as the PA. Here, a problem appears: how should we model such a channel? The intuitive idea is that the correlation between $H$ and $\hat{H}$ should be affected by the moving speed $v$, the time for UL and DL, as well as the antenna separation $d_\mathrm{a}$ between the PA and RA.

One way to evaluate such function is to measure $H$ and $\hat{H}$ under different system configurations, and calculate the normalized mean squared error (NMSE) of $H$ and $\hat{H}$. Followed by [19], experimental results in [20] and [42] show that an NMSE of around -10 dB can be obtained for speeds up to 50 km/h, with all measured prediction horizons up to 3$\lambda$, which is ten times longer than the limit for channel extrapolation. In [20], [21], [42] frequency division duplex (FDD) systems are considered, where dense enough DL channel estimation pilots with orthogonal frequency-division multiplexing (OFDM) are used. On the other hand, for TDD systems, the UL and DL frames need to be adjusted so that the estimation of $H$ can be as close as $\hat{H}$, as proposed and evaluated in [23]. However, such method would need to adapt UL and DL ratios for each user, which is complicated from the system design point of view. To mitigate this issue, an interpolation scheme is proposed in [23] which is suitable for different UL and DL ratios. Also, Kalman smoother for the interpolation of the PA for TDD system with a two-filter approach is proposed in [22], where the CSI quality of the DL can be improved such that the duration of DL can be extended remarkably. Moreover, it is shown that the correlation between $H$ and $\hat{H}$ would be

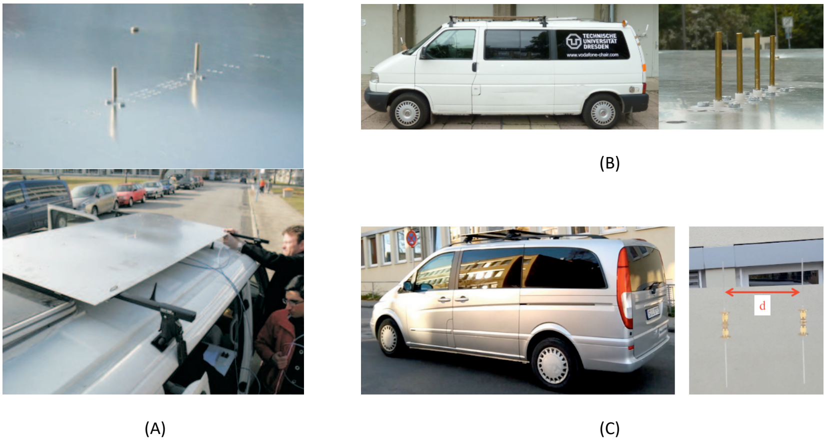


**Figure 2.1:** Illustrations of some testbed-based studies of the PA system. (A): Field trial of the PA setup with two in-line monopoles over a fairly large aluminium plane at 2.68 GHz, in Dresden, Germany (Source: ©2014 IEEE. Reprinted, with permission, from [43, Fig. 2]); (B): The linear array of four monopole antennas are deployed on the roof of a van at 2.53 GHz, in Dresden, Germany (Source: ©2017 IEEE. Reprinted, with permission, from [20, Fig. 5] and [42, Fig. 5]); (C): The drive tests with the PA scheme where two monopole antennas are mounted on the metallic plane at 2.18 GHz, in Stuttgart, Germany [21, Fig. 4].

reduced, if the PA and the RA are too close to each other, e.g., 0.2-0.4$\lambda$. Different ways to compensate for such coupling effect are proposed in [24], [43].

## 2.2 PA Validation by Testbed-based Experimental Evaluations

To validate the PA concept in practice, among the PA works mentioned above, some of them provide valuable testbed-based experiments as highlighted in the following.

### 2.2.1 The First Experiment of the PA

Along with the demonstration of the PA idea, studies in [19] provide, firstly, the experimental validation of the PA setup. A single-antenna transmitter is mounted on the top of a building with 55 m height. At the receiver side, two dipole antennas are deployed on the roof of a bus. The measurements are collected at the speed of 45-50 km/h in a residential place with buildings of 10-50 m height. Distances between the two dipole antennas are set to $\lambda/4$, $\lambda/2$, $\lambda$, $2\lambda$, and $3\lambda$ with $\lambda$ referring to the wavelength. Both LoS and NLoS are considered in the measurements.

The results of [19] show that the addition of an antenna, i.e., the PA, could realize prediction ranges 1) slightly below $\lambda/2$ for NLoS and 2) around $\lambda$ for the LoS, which are good enough for the requirements in LTE relay links for buses and trams.

### 2.2.2 Test in Dresden, Germany in 2014

In 2014, authors in [43] perform a field trial of the PA system in Dresden, Germany. The study is designed to mount two in-line thin $\lambda/4$ monopole antennas on the roof of a vehicle with around 50 km/h speed, and the system has a bandwidth of 20 MHz and carrier frequency 2.68 GHz, as shown in Fig. 2.1-(A). The BS has one single antenna and it is located at the top of a building with a height of 55 m. A large aluminum plane sheet is used in order to mitigate unexpected reflection and scattering and the refraction from the nonuniform roof.

Measurements are mainly focusing on the received signals for the PA and RA with/without coupling compensations. Here, both LoS and NLoS scenarios are considered. Finally, the temporal cross-correlation between the received signals for the PA and the RA is used as the main performance criterion.

From the test results, the mean cross-correlation between the received signals of the PA and RA is observed to remain high ($\geq 97\%$), after coupling compensation, for at least 3 times the wavelength in both LoS and NLoS scenarios, while the coupling compensation has the most remarkable benefits when the antenna separation is less than $\lambda$.

### 2.2.3 Test in Dresden, Germany in 2017

In 2017, a testbed-based study is designed in [20] and its follow-up work [42] in Dresden, Germany, with vehicle speed of 25-50 km/h at 2.53 GHz for both LoS and NLoS channels. As illustrated in Fig. 2.1-(B), a linear array of four monopole antennas are deployed on the roof of a van, and a metal sheet is placed below the antennas for an idealized local surrounding that is independent of the particular type of vehicle. With a focus on the UL channel, 16 BSs are deployed with two antennas at each of them, and they receive and record the OFDM signals from the vehicle.

The experiments in [20], [42] with different signal processing techniques validate the correlation-based analytical model, and prove that prediction accuracy of around $-13$ to $-7$ dB can be achieved, which is sufficient to support various transmission schemes such as precoding and spatial multiplexing.

### 2.2.4 Test in Stuttgart, Germany in 2018

In 2018, a field study is performed in Stuttgart, Germany, with a massive MIMO setup operating at 2.18 GHz [21]. As shown in Fig. 2.1-(C), two monopole antennas are deployed on the top of a car with a metallic plane with distance of 11 cm, 15 cm, and 42 cm. A 64-antenna array is located on the top of a building with a height of 20 m. The BS sends an OFDM waveform of 10 MHz at the carrier frequency of 2.18 GHz. For the measurements, the channels from the array to two RAs are stored in 50 frequency blocks at every 0.5 ms, along with their time stamps. These data are then used to evaluate the receiver noise power, which is part of the derivation of receive signal-to-noise ratio (SNR) and noise-free received signal power.

Results reveal that, at low/moderate speeds, the complex DL channels can be well predicted with an accuracy that enables maximum ratio transmission (MRT) BF with close to ideal BF gain for NLoS channels. This is the first time drive tests of the PA are performed for massive MIMO systems.

These testbed results verify the usefulness of the PA concept in MRs. However, to be practically implemented, MR standardization should be first specified.

## 2.3 Challenges and Difficulties

Previous studies have shown that deploying the PA system can provide significant performance gains in terms of, e.g., NMSE [20], [21], [42]. However, the realistic gains can be limited by different practical constraints. In this section, we discuss a number of challenges that have been partly addressed in this work.

### Lack of Analytical Model

In the literature, most PA studies rely on experimental measurements and simulations. This is sufficient for the validation purposes. However, to have a deeper understanding of the PA system, it is useful to develop analytical models. There are different statistical wireless channel models such as Rayleigh, Rice, Nakagami, and log-normal fading, as well as their combinations on multi-path and shadow fading components [44], [45]. Here, obtaining exact analytical model for the PA system may be difficult, but understanding the correlation between $H$ and $\hat{H}$ would be a good starting point.

### Spatial Mismatch

As addressed in, e.g., [23], [24], even assuming that the channel does not change over time and space, if the RA does not arrive in the same point as the PA, the actual channel for the RA would not be identical to the one experienced by the PA before. As an example in Fig. 1.1 with a TDD setup, consider one vehicle deploying two antennas on the roof with one PA positioned in the front of the moving direction and an RA aligned behind the PA. The idea of the data transmission model is that the PA first sends pilots at time $t$, then the BS estimates the channel and sends the data at time $t+\delta$ to the RA. Here, $\delta$ depends on the processing time at the BS. Then, we define $d$ as the effective distance between the position of the PA at time $t$ and the position of the RA at time $t+\delta$, as can be seen in Fig. 1.1. That is, $d$ is given by

$$d = |d_{\mathrm{a}} - d_{\mathrm{m}}| = |d_{\mathrm{a}} - v\delta|, \tag{2.1}$$

where $d_{\mathrm{m}}$ is the moving distance between $t$ and $t+\delta$, while $v$ is the velocity of the vehicle. To conclude, different values of $v$, $\delta$, $f_{\mathrm{c}}$ and $d_{\mathrm{a}}$ in (2.1) correspond to different values of $d$. We would like to find out how to connect $H$ and $\hat{H}$ as a function of $d$, and how different values of $d$ would affect system performance.

### Spectral Efficiency Improvement

In a typical PA setup, the spectrum is underutilized, and spectral efficiency could be further improved in case the PA could be used not only for channel prediction but also for data transmission. However, proper data transmission schemes need to be designed to make the best use of the PA.

### Temporal Correlation

The overhead from the UL-DL structure of the PA system would affect the accuracy of the CSI acquisition, i.e., the $\hat{H}$ obtained from PA would change over time. Basically, the slowly-fading channel is not always a realistic model for fast-moving users, since the channel may change by the environmental effects during a transmission block [46]–[48]. There are different ways to model the temporally-correlated channel, such as using the first-order Gauss-Markov process [47], [48].

### Estimation Error

There could be channel estimation error from UL [49], which would degrade the system performance. The assumption of perfect channel reciprocity in TDD ignores two important facts [50]: 1) the RF chains of UL and DL are separate circuits with possibly different impacts on the transmitted and received signals [50], [51], which is the so-called RF mismatch; 2) the interference profile at the transmitter and receiver sides are different [52]. These deviations are defined as reciprocity errors that invalidate the assumption of perfect reciprocity, and should be considered in the system design.

### Effects of Other Parameters

As mentioned in Fig. 1.1, different system parameters, such as the speed $v$, the antenna separation $d_\mathrm{a}$, and the control loop time $\delta$, would affect the system behavior by, e.g., spatial mismatch or antenna coupling. Our goal is to study the effect of these parameters and develop robust schemes which perform well for a broad range of their values.

## 2.4 Proposed Analytical Channel Model

Considering DL transmission in the BS-RA link, which is our main interest, the received signal is given by

$$Y = \sqrt{P} H X + Z. \tag{2.2}$$

Here, $P$ represents the average received power at the RA, while $X$ is the input message with unit variance, and $H$ is the fading coefficient between the BS and the RA. Also, $Z \sim \mathcal{CN}(0,1)$ denotes the identical and independently distributed (i.i.d.) complex Gaussian noise added at the receiver.

We denote the channel coefficient of the PA-BS UL by $\hat{H}$ and we assume that $\hat{H}$ is perfectly known by the BS. The result can be extended to the cases with imperfect CSI at the BS (see our work Paper B [53]). In this way, we use the spatial correlation model [54, p. 2642] [55, Eq. (3)]

$$\tilde{\boldsymbol{H}} = \boldsymbol{\Phi}^{1/2} \boldsymbol{H}_\varepsilon, \tag{2.3}$$

where

$$\tilde{\boldsymbol{H}} = \left[\begin{smallmatrix} \hat{H} \\ H \end{smallmatrix}\right] \tag{2.4}$$

is the channel matrix including both BS-PA channel $\hat{H}$ and BS-RA channel $H$ links. Here, $\boldsymbol{H}_\varepsilon$ has independent circularly-symmetric zero-mean complex Gaussian entries with unit variance, and $\boldsymbol{\Phi}$ is the channel correlation matrix.

In general, the spatial correlation of the fading channel depends on the distance between the RA and PA, which we denote by $d_\mathrm{a}$, as well as the angular spectrum of the radio wave pattern. If we use the classical Jakes' correlation model by assuming uniform angular spectrum, the $(i,j)$-th entry of $\boldsymbol{\Phi}$ is given by [56, Eq. 1]

$$\Phi_{i,j} = J_0\left((i-j) \cdot 2\pi d/\lambda\right). \tag{2.5}$$

Here, $J_0(\cdot) = \sum_{k=0}^{\infty} (-1)^k \left(z^2/4\right)^k / (k!)^2$ [57, p. 360] is the zeroth-order Bessel function of the first kind. Also, $\lambda = c/f_\mathrm{c}$ represents the wavelength where $c$ is the speed of light and $f_{\mathrm{c}}$ is the carrier frequency.

As discussed before, different values of $v$, $\delta$, $f_{\mathrm{c}}$ and $d_{\mathrm{a}}$ in (2.1) correspond to different values of $d$, which leads to different levels of channel spatial correlation (2.3)-(2.5).

Combining (2.3) and (2.5) with normalization, we have

$$H = \sqrt{1-\sigma^2}\hat{H} + \sigma q, \tag{2.6}$$

where $q \sim \mathcal{CN}(0,1)$ which is independent of the known channel value $\hat{H} \sim \mathcal{CN}(0,1)$, and $\sigma$ is a function of the spatial mismatch distance $d$.

From (2.6), for a given $\hat{H}$ and $\sigma \neq 0$, $|H|$ follows a Rician distribution, i.e., the probability density function (PDF) of $|H|$ is given by

$$f_{|H|\big|\hat{H}}(x) = \frac{2x}{\sigma^2} e^{-\frac{x^2+(1-\sigma^2)\hat{g}}{\sigma^2}} I_0\left(\frac{2x\sqrt{(1-\sigma^2)\hat{g}}}{\sigma^2}\right), \tag{2.7}$$

with $\hat{g} = |\hat{H}|^2$, and $I_n(x) = (x/2)^n \sum_{i=0}^{\infty} (x/2)^{2i} / \left(i!\Gamma(n+i+1)\right)$ being the $n$-th order modified Bessel function of the first kind, where $\Gamma(z) = \int_0^{\infty} x^{z-1}e^{-x}\mathrm{d}x$ denotes the Gamma function [57, p. 375]. Then, we define the channel gain between BS-RA as $g = |H|^2$. By changing variables from $H$ to $g$, the PDF of $f_{g|\hat{H}}$ is given by

$$f_{g|\hat{H}}(x) = \frac{1}{\sigma^2} e^{-\frac{x+(1-\sigma^2)\hat{g}}{\sigma^2}} I_0\left(\frac{2\sqrt{x(1-\sigma^2)\hat{g}}}{\sigma^2}\right), \tag{2.8}$$

which is non-central Chi-squared distributed, and the CDF is

$$F_{g|\hat{H}}(x) = 1 - Q_1\left(\sqrt{\frac{2(1-\sigma^2)\hat{g}}{\sigma^2}}, \sqrt{\frac{2x}{\sigma^2}}\right). \tag{2.9}$$

Here, $Q_1(\alpha, \beta)$ is Marcum $Q$-function and it is defined as [29, Eq. 1]

$$Q_1(\alpha, \beta) = \int_{\beta}^{\infty} x e^{-\frac{x^2+\alpha^2}{2}} I_0(x\alpha)\mathrm{d}x, \tag{2.10}$$

where $\alpha, \beta \geq 0$.

We study the system performance in temporally-correlated conditions, i.e., when $H$ is not the same as $\hat{H}$ even at the same position. Particularly, using the same model as in [47, Eq. 2], we further develop our channel model (2.6) as

$$H_{k+1} = \beta H_k + \sqrt{1-\beta^2} z, \tag{2.11}$$

for each time slot $k$, where $z \sim \mathcal{CN}(0,1)$ is a Gaussian noise, which is uncorrelated with $H_k$. Also, $\beta$ is a known correlation factor which represents two successive channel realizations dependencies by $\beta = \mathbb{E}\{H_{k+1}H_k^*\}/\mathbb{E}\{|H_k|^2\}$. Substituting (2.11) into (2.6), we have

$$H_{k+1} = \beta\sqrt{1-\sigma^2}\hat{H}_k + \beta\sigma q + \sqrt{1-\beta^2}z = \beta\sqrt{1-\sigma^2}\hat{H}_k + w. \tag{2.12}$$

Here, to simplify the calculation, $\beta\sigma q + \sqrt{1-\beta^2}z$ is equivalent to a new Gaussian variable $w \sim \mathcal{CN}\left(0, (\beta\sigma)^2 + 1 - \beta^2\right)$. Moreover, we can follow the same approach as in [58] to add the effect of estimation error of $\hat{H}$ as an independent additive Gaussian variable whose variance is given by the accuracy of CSI estimation.

## 2.5 First-Order Marcum Q-Function and Semi-Linear Approximation

First-order Marcum $Q$-function (2.10) is used in various problem formulations. However, from (2.10) it can be observed that the function is not an easy-to-handle function with modified Bessel function, double parameters ($\alpha$ and $\beta$), and the integral shape.

In the literature, Marcum $Q$-function has appeared in different problem formulations, such as statistics/signal detection [59], and in performance analysis of various setups, such as temporally correlated channels [47], spatial correlated channels [60], free-space optical (FSO) links [61], relay networks [62], as well as cognitive radio and radar systems [63]–[83]. However, in these applications, the presence of Marcum $Q$-function makes the mathematical analysis challenging, because it is not easy to manipulate with no closed-form expressions especially when it appears in parameter optimizations and integral calculations. Therefore, several methods have been developed in [29], [84]–[95] to bound/approximate Marcum $Q$-function. For example, modified forms of the function are proposed in [84], [85], while exponential-type bounds are derived in [86], [87] which are good for the analysis at high SNRs. Other types of bounds are expressed by, e.g., error function [92] and Bessel functions [93]–[95]. Some alternative methods have been also proposed in [29], [88]–[91]. Although each of these approximation/bounding techniques are fairly tight for their considered problem formulation, they are still based on hard-to-deal functions, or have complicated summation/integration structures, which may be not easy to deal with in e.g., integral calculations and parameter optimizations.

We present our semi-linear approximation of the CDF in the form of $y(\alpha, \beta) = 1 - Q_1(\alpha, \beta)$. The idea of this proposed approximation is to use one point and its corresponding slope at that point to create a line approximating the CDF. The approximation method is summarized in Lemma 1 as follows.

**Lemma 1.** *The CDF $y(\alpha, \beta) = 1 - Q_1(\alpha, \beta)$ can be semi-linearly approximated as*

$Y(\alpha,\beta) \simeq \mathcal{Z}(\alpha,\beta)$ *where*

$$\mathcal{Z}(\alpha,\beta) = \begin{cases} 0, & \text{if } \beta < c_1 \\ \frac{\alpha+\sqrt{\alpha^2+2}}{2} e^{-\frac{1}{2}\left(\alpha^2+\left(\frac{\alpha+\sqrt{\alpha^2+2}}{2}\right)^2\right)} \times & \\ \quad I_0\left(\alpha\frac{\alpha+\sqrt{\alpha^2+2}}{2}\right) \times \left(\beta - \frac{\alpha+\sqrt{\alpha^2+2}}{2}\right) + & \\ \quad 1 - Q_1\left(\alpha, \frac{\alpha+\sqrt{\alpha^2+2}}{2}\right), & \text{if } c_1 \leq \beta \leq c_2 \\ 1, & \text{if } \beta > c_2, \end{cases} \tag{2.13}$$

*with*

$$c_1(\alpha) = \max\left(0, \frac{\alpha+\sqrt{\alpha^2+2}}{2} + \frac{Q_1\left(\alpha, \frac{\alpha+\sqrt{\alpha^2+2}}{2}\right) - 1}{\frac{\alpha+\sqrt{\alpha^2+2}}{2} e^{-\frac{1}{2}\left(\alpha^2+\left(\frac{\alpha+\sqrt{\alpha^2+2}}{2}\right)^2\right)} I_0\left(\alpha\frac{\alpha+\sqrt{\alpha^2+2}}{2}\right)}\right), \tag{2.14}$$

$$c_2(\alpha) = \frac{\alpha+\sqrt{\alpha^2+2}}{2} + \frac{Q_1\left(\alpha, \frac{\alpha+\sqrt{\alpha^2+2}}{2}\right)}{\frac{\alpha+\sqrt{\alpha^2+2}}{2} e^{-\frac{1}{2}\left(\alpha^2+\left(\frac{\alpha+\sqrt{\alpha^2+2}}{2}\right)^2\right)} I_0\left(\alpha\frac{\alpha+\sqrt{\alpha^2+2}}{2}\right)}. \tag{2.15}$$

*Proof.* See Paper B [53, Sec. II]. ■

Moreover, we can make some second level approximations considering different ranges of $\alpha$ to further simplify notations. For more details, see [53], i.e., the appended Paper B.

One example result of the proposed approximation can be seen in Fig. 2.2 with $\alpha$ set to 2. We can observe that Lemma 1 is tight for moderate values of $\beta$. Note that the proposed approximations are not tight at the tails of the CDF. However, as observed in [29], [47], [59]–[74], [84]–[95], in different applications, Marcum $Q$-function is typically combined with other functions which tend to zero in the tails of the CDF. In such cases, the inaccuracy of the approximation at the tails does not affect the tightness of the final analysis.

For example, it can simplify integrals such as

$$G(\alpha,\rho) = \int_{\rho}^{\infty} e^{-nx} x^m \left(1 - Q_1(\alpha, x)\right) \mathrm{d}x \quad \forall n, m, \alpha, \rho > 0. \tag{2.16}$$

Such an integral has been observed in various applications, e.g., in [63, Eq. 1], [72, Eq. 2], [73, Eq. 1], [74, Eq. 3], and [91, Eq. 1]. However, depending on the values of

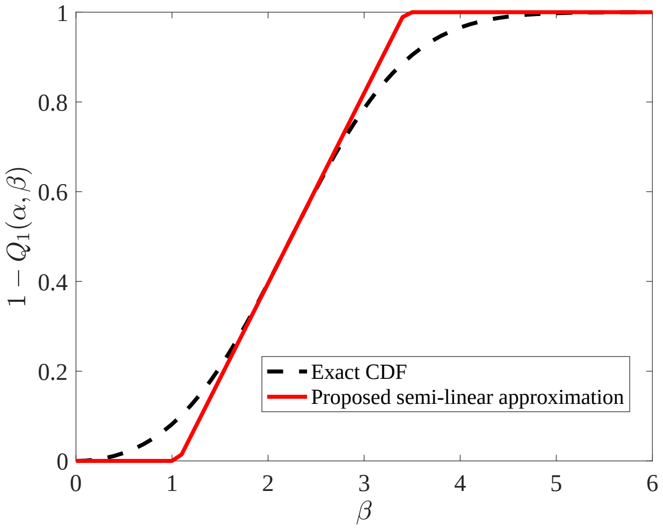


**Figure 2.2:** The illustration of proposed semi-linear approximation, $\alpha = 2$.

$n, m$ and $\rho$, (2.16) may have no closed-form expression.

Another example of integral calculation is

$$T(\alpha, m, a, \theta_1, \theta_2) = \int_{\theta_1}^{\theta_2} e^{-mx} \log(1 + ax) Q_1(\alpha, x) \mathrm{d}x \quad \forall m > 0, a, \alpha, \tag{2.17}$$

with $\theta_2 > \theta_1 \geq 0$, which does not have a closed-form expression for different values of $m, a, \alpha$. This integral is interesting as it is often used to analyse the expected performance of outage-limited systems, e.g, [63], [86], [91], [96]. Then, as we show in Paper B [53], the developed semi-linear approximation makes it possible to derive simple closed-form expressions for such integration calculations.

Finally, the proposed semi-linear approximation can be used for the rate adaptation scheme developed in the PA system. For more details, please refer to Chapter 3 as well as Paper B [53, Sec. II].

# CHAPTER 3

## Performance Enhancement Using Resource Allocation in PA Systems

Resource allocation plays an important role in communication systems as a way of optimizing the assignment of available resources to achieve network design objectives. In the PA system, resource allocation can be deployed to mitigate different challenges mentioned in Chapter 2. In this chapter, we develop various resource allocation schemes for the PA system under different practical constraints.

## 3.1 Rate Adaptation in the Classic PA Setup

In this section, we propose a rate adaptation scheme to mitigate the spatial mismatch problem. Here, the classic setup means the PA is only used for channel prediction, not for data transmission. We assume that $d_{\mathrm{a}}$, $\delta$ and $\hat{g}$ are known at the BS. It can be seen from (2.8) that $f_{g|\hat{H}}(x)$ is a function of the speed $v$. For a given $v$, the distribution of $g$ is known at the BS, and a rate adaption scheme can be performed to improve the system performance.

The data is transmitted with rate $R^*$ nat per channel use (npcu). If the instantaneous realization of the channel gain supports the data rate, i.e., $\log(1+gP) \geq R^*$, the data can be successfully decoded, otherwise outage occurs. Hence, the outage probability in each time slot is obtained as $\Pr(\text{Outage}|\hat{H}) = F_{g|\hat{H}}\left(\left(e^{R^*}-1\right)/P\right)$. Considering slotted communication in block fading channels, where $\Pr(\text{Outage}) > 0$ varies with different fading models, throughput [97, p. 2631], [98, Th. 6], [99, Eq. 9] defined as the data rate times the successful decoding probability, i.e., the expected data rate successfully received by the receiver, is an appropriate performance metric. Hence, the rate adaptation problem of maximizing the throughput in each time slot, with given $v$ and $\hat{g}$, can be expressed as

$$\begin{aligned} R_{\mathrm{opt}|\hat{g}} &= \underset{R^* \geq 0}{\operatorname{argmax}} \left\{ \left(1 - \Pr\left(\log(1+gP) < R^*\right)\right) R^* \right\} \\ &= \underset{R^* \geq 0}{\operatorname{argmax}} \left\{ \left(1 - \Pr\left(g < \frac{e^{R^*}-1}{P}\right)\right) R^* \right\} \\ &= \underset{R^* \geq 0}{\operatorname{argmax}} \left\{ \left(1 - F_{g|\hat{H}}\left(\frac{e^{R^*}-1}{P}\right)\right) R^* \right\}. \end{aligned} \tag{3.1}$$

Also, defining the expectation operator by $\mathbb{E}\{\cdot\}$, the expected throughput is obtained by $\mathbb{E}\left\{\left(1 - F_{g|\hat{H}}\left(\left(e^{R_{\mathrm{opt}|\hat{g}}}-1\right)/P\right)\right) R_{\mathrm{opt}|\hat{g}}\right\}$ with expectation over $\hat{g}$.

Using (2.9), (3.1) is simplified as

$$R_{\mathrm{opt}|\hat{g}} = \underset{R^* \geq 0}{\operatorname{argmax}} \left\{ Q_1\left(\sqrt{\frac{2\hat{g}(1-\sigma^2)}{\sigma^2}}, \sqrt{\frac{2(e^{R^*}-1)}{P\sigma^2}}\right) R^* \right\}. \tag{3.2}$$

In general, (3.2) does not have a closed-form solution. For this reason, in [100] (the appended Paper A) and [53] (the appended Paper B) we propose different approximations for the optimal data rate maximizing the instantaneous throughput.

## 3.2 Hybrid Automatic Repeat Request in the PA Systems

HARQ is a well-known approach to improve the data transmission reliability and efficiency. The main idea of HARQ is to retransmit the message that experienced poor channel conditions in order to reduce the outage probability [99], [101], [102]. Here, we define that outage occurs when the transmitted message can not be decoded at the receiver. For the Rayleigh block fading channel, infinite power is required to achieve zero outage probability for all realizations. Hence, we replace the strict outage constraint by a more realistic requirement, where a transmission is successful as long as the message can always be decoded by the receiver with probability $\epsilon$. We define $\epsilon$ as a parameter of the system outage tolerance.

Outage-constrained power allocation problem in HARQ system is studied, e.g, in [103] with perfect CSI assumption, in [104] with cooperative decode-and-forward automatic repeat request (ARQ) relaying under packet-rate fading channels, and in [105], [106] with power allocation schemes aiming at minimizing average power for HARQ systems. Also, in block fading scenario, authors in [107] study the outage-limited performance of different HARQ protocols. Moreover, the outage-constrained power optimization for the repetition time diversity (RTD) and fixed-length coding incremental redundancy (INR) HARQ protocols are investigated in [108] and [109], respectively. Assuming that the channel changes in each re-transmission, authors in [110] develop power allocation schemes with basic ARQ. Finally, a linear-programming approach with a buffer cost constraint is proposed in [111] to solve the power adaptive problem in HARQ systems where the power is adapted based on the received CSI.

As the PA system includes the feedback link, i.e., from the PA to the BS, HARQ can be supported by the PA structure in the moving scenarios. That is, the BS could potentially adjust its transmit rate/power based on the feedback from the PA. In this way, it is expected that the joint implementation of the PA system and the HARQ scheme can improve the efficiency and reliability of outage-constrained systems. There are limited studies on deploying HARQ in moving scenarios, i.e., when the channel changes quickly over time compared to the feedback delay. Particularly, [112] investigated the performance of basic ARQ and INR protocols in fast-fading channels where a number of channel realizations are experienced in each retransmission round. Also, [113] studied the performance of INR over double Rayleigh channels, a common model for the fading amplitude of vehicle-to-vehicle communication systems. However, both [112] and [113] deal with the same channel PDF for different re-transmission rounds, which has limited contribution for the spatial/temporal variation of channel in vehicle communications.

In the classic PA setup, the spectrum is underutilized, and the spectral efficiency could be further improved in the case that the PA could be used not only for channel prediction, but also for data transmission. We address these challenges by implementing HARQ-based protocols in PA systems as follows.

As seen in Fig. 3.1, the BS first sends pilots as well as the encoded data with certain initial parameters, e.g., power or rate depending on the problem formulation, to the PA. Then, the PA estimates the channel from the received pilots. At the same time, the PA tries to decode the signal. If the message is correctly decoded, an acknowledgment (ACK) is fed back to the BS, and the data transmission stops. Otherwise, the PA sends both a negative acknowledgment (NACK) and high accuracy quantized CSI feedback. The number of quantization bits are large enough such that we can assume the BS to have perfect CSI. With NACK, in the second transmission round, the BS transmits the message to the RA with adapted power/rate which is a function of the instantaneous channel quality in the first round. The outage occurs if the RA can not decode the message at the end of the second round.

In the following section, we develop an outage-constrained power allocation scheme in the HARQ-based PA system. The related study about delay-limited average rate optimization in the HARQ-based PA system can be found in [114] (the appended Paper D).

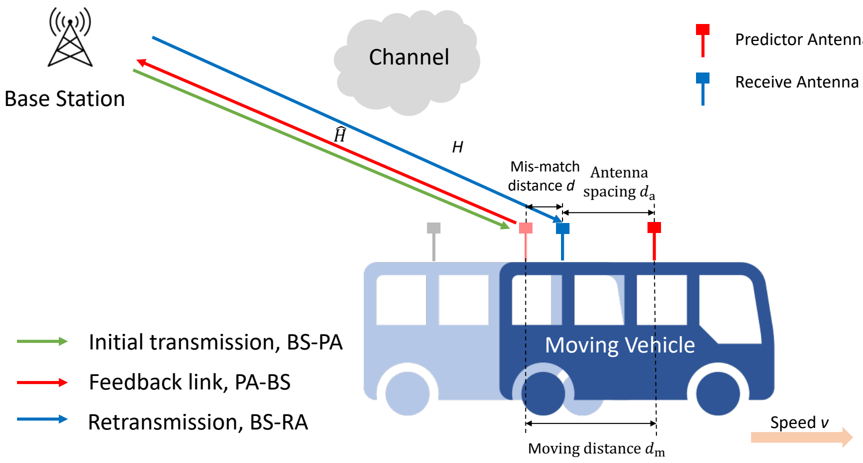


**Figure 3.1:** The PA concept with HARQ.

## 3.3 Outage-constrained Power Allocation in the HARQ-based PA Systems

As seen in Fig. 3.2, without CSI, at $t_1$ the BS sends pilots as well as the encoded data with a certain initial rate $R$ and power $P_1$ to the PA. At $t_2$, the PA estimates the channel $\hat{H}$ from the received pilots. At the same time, the PA tries to decode the signal. If the message is correctly decoded, i.e., $R \leq \log(1+\hat{g}P_1)$, an ACK is fed back to the BS at $t_3$, and the data transmission stops. Otherwise, the PA sends both a NACK and high accuracy quantized CSI feedback about $\hat{H}$. With NACK, in the second transmission round at time $t_4$, the BS transmits the message to the RA with power $P_2$, which is a function of the instantaneous channel quality $\hat{g}$. The outage occurs if the RA can not decode the message at the end of the second round.

Let $\epsilon$ be the outage probability constraint. Here, we present the results for the cases with RTD and INR HARQ protocols. With an RTD protocol, the same signal (with possibly different power) is sent in each retransmission round, and the receiver performs maximum ratio combining of all received copies of the signal. With INR, on the other hand, new redundancy bits are sent in the retransmissions, and the receiver decodes the message by combining all received signals [105], [109], [111].

Considering Rayleigh fading conditions with $f_{\hat{g}}(x) = e^{-x}$, the outage probability

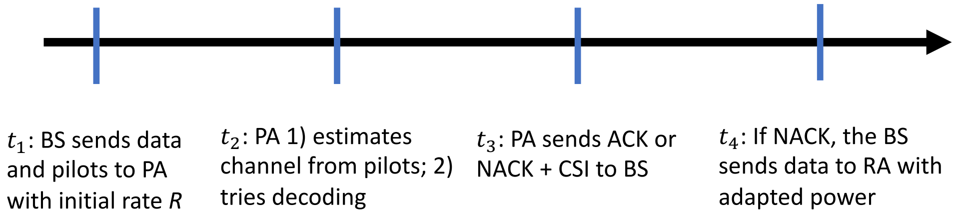


**Figure 3.2:** Time structure for the proposed outage-constrained power allocation in the HARQ-based PA system from Paper C [115].

at the end of Round 1 is given by

$$\Pr(\text{Outage, Round 1}) = \Pr\left\{R \leq \log\left(1+\hat{g}P_1\right)\right\} = \Pr\left\{\hat{g} \leq \frac{e^R-1}{P_1}\right\} = 1 - e^{-\frac{\theta}{P_1}}, \tag{3.3}$$

where $\theta = e^R - 1$. Then, using the results of, e.g., [105, Eq. 7, 18] on the outage probability of the RTD- and INR-based HARQ protocols, the power allocation problem for the proposed HARQ-based PA system can be stated as [115] (the appended Paper C)

$$\begin{aligned}
\min_{P_1,P_2} \quad & \mathbb{E}_{\hat{g}}\left[P_{\text{tot}}|\hat{g}\right] \\
\text{s.t.} \quad & P_1, P_2 > 0, \\
& P_{\text{tot}}|\hat{g} = \left[P_1 + P_2(\hat{g}) \times \mathcal{I}\left\{\hat{g} \leq \frac{\theta}{P_1}\right\}\right],
\end{aligned} \tag{3.4}$$

with

$$F_{g|\hat{g}}\left\{\frac{\theta - \hat{g}P_1}{P_2(\hat{g})}\right\} = \epsilon, \quad \text{for RTD} \tag{3.5}$$

$$F_{g|\hat{g}}\left\{\frac{e^{R-\log(1+\hat{g}P_1)}-1}{P_2(\hat{g})}\right\} = \epsilon, \quad \text{for INR.} \tag{3.6}$$

Here, $P_{\text{tot}}|\hat{g}$ is the total instantaneous transmission power for two transmission rounds (i.e., one retransmission) with the given $\hat{g}$, and we define $\bar{P} \doteq \mathbb{E}_{\hat{g}}\left[P_{\text{tot}}|\hat{g}\right]$ as the expected power, averaged over $\hat{g}$. Moreover, $\mathcal{I}(x) = 1$ if $x > 0$ and $\mathcal{I}(x) = 0$ if $x \leq 0$. Also, $\mathbb{E}_{\hat{g}}[\cdot]$ represents the expectation operator over $\hat{g}$. Here, we ignore the peak power constraint and assume that the BS is capable for sufficiently high transmission powers. Finally, (3.4)-(3.6) come from the fact that, with our proposed scheme, $P_1$ is fixed and optimized with no CSI at the BS and based on average system performance.

On the other hand, $P_2$ is adapted continuously based on the instantaneous CSI.

Using (3.4), the required power in Round 2 is given by

$$P_2(\hat{g}) = \frac{\theta - \hat{g}P_1}{F^{-1}_{g|\hat{g}}(\epsilon)}, \tag{3.7}$$

for the RTD, and

$$P_2(\hat{g}) = \frac{e^{R-\log(1+\hat{g}P_1)} - 1}{F^{-1}_{g|\hat{g}}(\epsilon)}, \tag{3.8}$$

for the INR, where $F^{-1}_{g|\hat{g}}(\cdot)$ is the inverse of the CDF given in (2.9). Note that $F^{-1}_{g|\hat{g}}(\cdot)$ is a complicated function of $\hat{g}$, and consequently, it is not possible to express $P_2$ in closed-form. For this reason, one can use [29, Eq. 2, 7]

$$\begin{aligned}
&Q_1(s,\rho) \simeq e^{\left(-e^{\mathcal{I}(s)}\rho^{\mathcal{J}(s)}\right)},\\
&\quad \mathcal{I}(s) = -0.840 + 0.327s - 0.740s^2 + 0.083s^3 - 0.004s^4,\\
&\quad \mathcal{J}(s) = 2.174 - 0.592s + 0.593s^2 - 0.092s^3 + 0.005s^4,
\end{aligned} \tag{3.9}$$

to approximate $F_{g|\hat{g}}$ and consequently $F^{-1}_{g|\hat{g}}(\epsilon)$. In this way, (3.7) and (3.8) can be approximated as

$$P_2(\hat{g}) = \Omega\left(\theta - \hat{g}P_1\right), \tag{3.10}$$

for the RTD, and

$$P_2(\hat{g}) = \Omega\left(e^{R-\log(1+\hat{g}P_1)} - 1\right), \tag{3.11}$$

for the INR, where

$$\Omega(\hat{g}) = \frac{2}{\sigma^2}\left(\frac{\log(1-\epsilon)}{-e^{\mathcal{I}\left(\sqrt{\frac{2\hat{g}(1-\sigma^2)}{\sigma^2}}\right)}}\right)^{-\frac{2}{\mathcal{J}\left(\sqrt{\frac{2\hat{g}(1-\sigma^2)}{\sigma^2}}\right)}}. \tag{3.12}$$

Thus, for different HARQ protocols, we can express the instantaneous transmission power of Round 2, for every given $\hat{g}$ in closed form. Then, the power allocation problem (3.4) can be solved numerically. However, (3.12) is still complicated and it is not possible to solve (3.4) in closed-form. For this reason, we propose an approximation scheme to solve (3.4) as follows.

Let us initially concentrate on the RTD protocol. Then, combining (3.4) and (3.7), the expected total transmission power is given by

$$\bar{P}_{\text{RTD}} = P_1 + \int_0^{\theta/P_1} e^{-x}P_2\text{d}x = P_1 + \int_0^{\theta/P_1} e^{-x}\frac{\theta - xP_1}{F^{-1}_{g|x}(\epsilon)}\text{d}x. \tag{3.13}$$

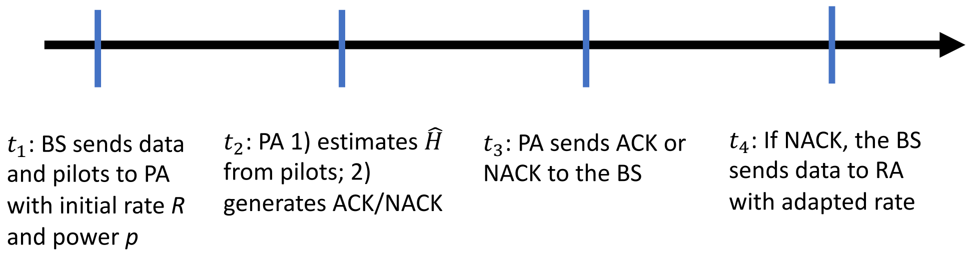


**Figure 3.3:** Time structure for the proposed delay-limited average rate optimization in the HARQ-based PA system.

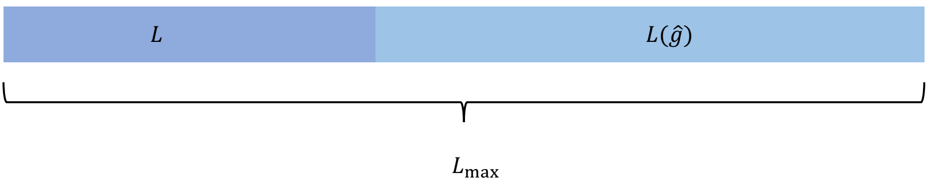


**Figure 3.4:** Illustration of the block length for two transmissions from Paper D [114].

Then, in Paper C [115, Theorem 1] we derive the minimum required power in Round 1 and the average total power consumption.

To study the performance of the INR, we can use Jensen's inequality and the concavity of the logarithm function [116, Eq. 30]

$$\frac{1}{n}\sum_{i=1}^{n}\log(1+x_i) \leq \log\left(1+\frac{1}{n}\sum_{i=1}^{n}x_i\right), \tag{3.14}$$

and derive the closed-form expressions for the minimum required power following the similar steps as for the RTD (see Paper C [115, Sec. III B]) for detailed discussions).

## 3.4 Delay-limited Average Rate Optimization in the HARQ-based PA Systems

In this section, we develop an HARQ-based scheme in delay-limited PA systems. The goal is to maximize the delay-constrained average rate in the presence of imperfect CSI as well as spatial mismatch.

The time structure shown in Fig. 3.3 is similar to Fig. 3.2 except that the power is replaced by rate. As shown in Fig. 3.4, let us denote the maximum acceptable delay constraint by $L_{\max}$ channel use (CU). Also, we denote the block length allocated to the first and the second transmission signals by $L$ and $L(\hat{g})$, respectively. Here, $L$

is optimized based on average performance, and $L(\hat{g})$ is based on the instantaneous channel quality $\hat{g}$. This is because the initial transmission to the PA is performed based on no CSIT at the BS. However, in the second round, the transmission length is adapted based on the instantaneous channel quality $\hat{g}$ available at the BS. In the following, we optimize the average rate in the presence of variable-length coding and maximum delay constraint.

Let us denote the initial rate by $R = K/L$ npcu, where $K$ is the number of nats per codeword. Then, in the first transmission, if the instantaneous channel gain supports the rate, i.e., $R < \log(1 + \hat{g}p)$ or equivalently, $\hat{g} > \theta/p$ where $\theta = e^R - 1$, an ACK is sent back to the BS and the transmission stops. On the other hand, if $R > \log(1 + \hat{g}p)$, an NACK as well as the instantaneous channel gain $\hat{g}$ are sent back to the BS. Then, in Round 2, we determine the required rate as

$$R(\hat{g}) = \log(1 + \hat{g}p) = \frac{K}{L + L(\hat{g})}, \tag{3.15}$$

which is equivalent to

$$L(\hat{g}) = \frac{K}{\log(1 + \hat{g}p)} - L. \tag{3.16}$$

Let us denote $R_{\min} = K/L_{\max}$ which is limited by the delay constraint $L_{\max}$. If $L(\hat{g}) + L > L_{\max}$ leading to $\hat{g} < \left(e^{R_{\min}} - 1\right)/p$, and no signal is sent in the second round because the maximum delay constraint can not be satisfied. Otherwise, if $\hat{g} > \left(e^{R_{\min}} - 1\right)/p$, we send a redundancy sub-codeword with length $L(\hat{g})$.

In this way, the average rate, for given $\hat{g}$, is given by

$$\eta|\hat{g} = R\mathcal{I}\left\{\hat{g} > \frac{\theta}{p}\right\} + \log(1 + \hat{g}p)\mathcal{I}\left\{\frac{\theta_{\min}}{p} \leq \hat{g} \leq \frac{\theta}{p}, \mathcal{A}\right\}. \tag{3.17}$$

Here, $\theta_{\min}$ is defined as $\theta_{\min} = e^{R_{\min}} - 1$. Also, $\mathcal{I}(x)$ is the indicator function and $\mathcal{A}$ is the event that the message is decoded in the second round. Note that, with the rate allocation scheme of (3.15), it is straightforward to show that $\mathcal{A}$ occurs if and only if $g \geq \hat{g}$. This is because $g \geq \hat{g}$, we have $\log(1 + gp) \geq \log(1 + \hat{g}p)$. This means that $R(\hat{g})$ is supported by the instantaneous channel gain $g$ in the second round. Hence, $\mathcal{I}(\mathcal{A}) = 1$. On the other hand, if the message is successfully decoded in the second round, we have

$$\begin{aligned}
&L\log(1+\hat{g}p)+L(\hat{g})\log(1+gp)\geq K\\
&\overset{(a)}{\Leftrightarrow} L\log(1+\hat{g}p)+\frac{K}{\log(1+\hat{g}p)}\log(1+gp)\geq K\\
&\Leftrightarrow \log(1+gp)\geq\frac{K-L\log(1+\hat{g}p)}{\frac{K}{\log(1+\hat{g}p)}-L}\\
&\Leftrightarrow \log(1+gp)\geq\log(1+\hat{g}p)\Leftrightarrow g\geq\hat{g}.
\end{aligned} \tag{3.18}$$

Here, $(a)$ is obtained by (3.16).

In this way, (3.17) can be rewritten as

$$\eta|\hat{g}=R\mathcal{I}\left\{\hat{g}>\frac{\theta}{p}\right\}+\log(1+\hat{g}p)\mathcal{I}\left\{\frac{\theta_{\min}}{p}\leq\hat{g}\leq\frac{\theta}{p},g\geq\hat{g}\right\}. \tag{3.19}$$

Finally, by averaging the system performance over all possible $\hat{g}$, we can obtain the average rate as presented in [114], i.e., the appended Paper D.

## 3.5 Adaptive Delay Transmission

Knowing the vehicle speed, the transmission delay can be dynamically adapted as a function of the antennas' distance and vehicle speed, such that the RA receives the data at the same point as the PA sending pilots. In this case, there is potentially no spatial mismatch, at the cost of extra transmission delay. However, the delay adaptation method is applicable only for a range of vehicle speeds limited by the access point's minimum required processing delay, and while it could improve the performance of the BS-MR link, it gives interference to the network which is not desirable. Also, cellular technologies only allow for limited transmission time interval granularity, and in practice, there would be residual mispointing.

In [117], i.e., the appended Paper E, we study the performance of adaptive delay, and compare its performance with various benchmark schemes in urban and rural environments.

# CHAPTER 4

## Towards Practical MRs: Cooperative Systems at MmWave

In practice, the deployment of MRs may face various challenges. Nevertheless, recent developments of advanced technologies, such as (massive) MIMO, BF, cooperative transmission, and RIS, provide more potentials to further improve the efficiency and reliability of MRs at the presence of rapidly-changing channels and dynamic blockages. These technologies would benefit from the context information of the system, e.g., the better CSIT obtained from the PA, the vehicle speed, the position of vehicle and dynamic blockers, to improve the communication performance.

In this chapter, schemes based on these technical enablers are presented. The main focus here is to present the system setup and the main method/algorithm, whereas the simulation results are described in details in appended Papers F-G.

## 4.1 Massive MIMO Beamforming-based PA Systems

Due to spatial mismatch, massive MIMO adaptive BF schemes based on CSIT, such as MRT and zero-forcing (ZF), suffer from BF mis-pointing and can benefit from the PA [23]. The left part of Fig. 4.1 illustrates BF mispointing for MRT BF, in an NLoS multi-path propagation scenario that is likely to be encountered in an urban environment. When MRT BF is used in a Rayleigh two-dimensional propagation environment, the BF pattern is close to a Bessel function, with side lobes every half wavelength. Hence, even a small spatial mismatch implies a strong degradation in the amount of the received power. As illustrated in the right part of Fig. 4.1, Discrete Fourier Transform (DFT)-based beamforming also suffers from BF mis-pointing, but

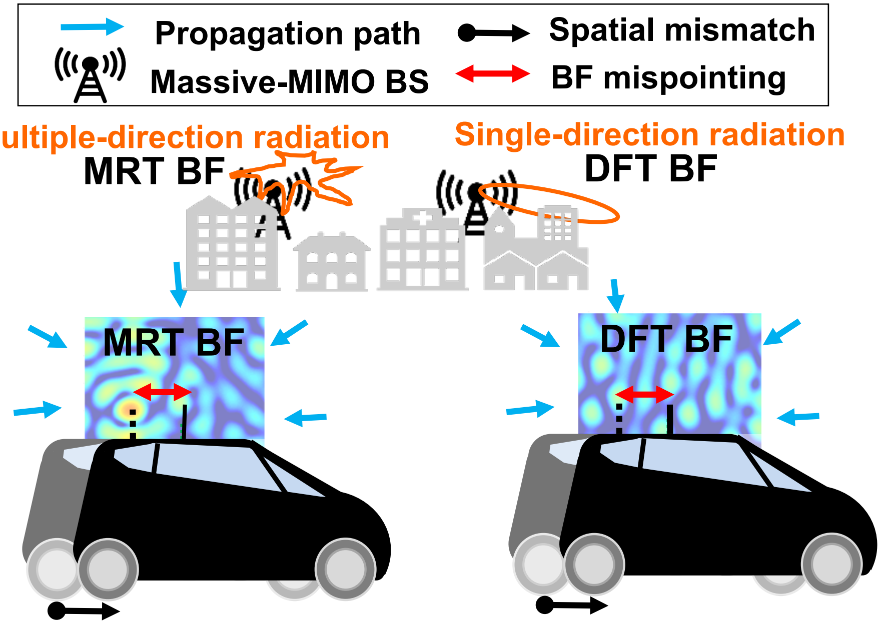


**Figure 4.1:** Illustration of massive MIMO schemes in PA systems with spatial mismatch [117] (the appended Paper E).

in a less severe manner. Indeed, on one side, MRT BF adapts to each individual path and is very sensitive to CSIT errors, whereas DFT BF forms a large beam towards a single direction, and is therefore less sensitive to CSIT errors.

Thanks to the PA, BF can be used without mispointing effect [23], to improve the spectral efficiency and the energy efficiency of the network, especially when the network is highly loaded with numerous moving cars [118] or high speed trains [119]. However, as explained previously, the PA alone suffers from residual spatial mismatch when the velocity, the PA spacing and the delay do not match. In this case, a prediction with zero residual spatial mismatch could be obtained by filtering and interpolating multiple measurements that suffer from residual spatial mismatch [120]. Recently, such schemes, with low complexity, and intended for implementation and on-line running on real BSs have been designed [22], [42]. Finally, experimental measurements [21] with a car and a 64 antenna-element massive MIMO BS in NLoS in an urban environment, and with various PA spacing values, have shown that the received power for MRT BF with PA based prediction is close to the one obtained with ideal prediction. They also show that the received powers of both MRT BF and ZF BF are improved by an order of magnitude with PA-based prediction, even when the PA spacing (i.e. the spatial mismatch to be compensated) is as large as three wavelengths.

## 4.2 Dynamic Blockage Avoidance

### 4.2.1 Background: Encounter Blockage at mmW

Suppose that, sitting in a vehicle driving in a highway, you are watching Game of Thrones, and your smart phone gets disconnected. In five years, this will bring huge dissatisfaction for the users, leading to poor rating for the network provider. Particularly, in the B5G era, users sitting in vehicles expect the same QoS as they have at home. Such use-cases with wireless communication to high-speed trains, busses, trams and cars are normally referred to as IoV.

To increase the data rate, different methods are considered, among which network densification and mmw communications are the dominant ones. Network densification refers to the deployment of multiple multi-antenna BSs of different types providing more resource blocks per area. Particularly, it is expected that soon small cells will be densely deployed to assist the existing macro BSs. On the other hand, mmw transmission offers wide bands and simplifies multi-antenna communications. However, it has inherent physical issues limiting its availability; Along with sensitivity to atmospheric variations, mmw transmission experiences poor propagation characteristics and has high LoS path loss. For these reasons, it is foreseen that mmw-enabled small cells will be deployed at low heights, e.g., on lamp post, with a short coverage range. With a low antenna height, however, the probability of blockage increases.

This is important because the mmw signals suffer from high penetration loss/low diffraction from objects and are significantly deteriorated by blockage. Therefore, to guarantee uninterrupted high-rate communications, it is preferred to avoid blockage.

With stationary/low mobility networks, one can well learn the network deployment and avoid (semi-)static blockages (such as buildings, trees, human bodies) via different resource association or cooperative communication schemes [121]. Alternatively, back-up NLoS links can be found by beam-sweeping during the initial beam training phase and, if a LoS link is blocked, the connection can be switched to the back-up link(s).

The problem, however, becomes more challenging when moving, e.g., moving networks with high-speed vehicles driving in highways. First, the back-up NLoS solution is not of interest because, along with signal attenuation, 1) good reflectors (building, etc.) are rare in highways, and 2) compared to urban scenario with rich scattering, such back-up links sustain for a shorter period. Second, considering low-height small cells in highways, the blockers are mainly busses and trucks passing by the cars. Thus, probabilistic blockage prediction or (machine learning-based) deployment learning methods may not cope well with the dynamics of the network at high speeds/frequencies. This is specially because not only the blockage results in excessive signal-to-interference-plus-noise ratio (SINR) degradation, but also the system performance is considerably affected by the channel aging phenomena where with high speeds the CSIT soon becomes inaccurate.

### 4.2.2 Existing Methodologies

Typical CSIT acquisition and blockage prediction schemes, designed for static networks, fail to work well in high speeds. As a result, one may need to switch to CSIT-free or diversity-based schemes at the cost of reliability and data rate. In the last few years, a number of methods such as Kalman prediction and PA [19] have been developed to improve the small-scale channel prediction quality in vehicle communications. However, 1) the performance of these methods drops quickly as the vehicle speed/frequency increases or the spatial mismatch occurs and 2) they can not avoid dynamic blockage which leads to considerable SINR drop.

Also, other alternative techniques such as prediction of the environment channel and CSIT adaptation based on the location information of the user equipment (UE) may be inaccurate with high information exchange overhead. With this background, to enable high-rate reliable IoV communications, we need methods to avoid not only the temporal blockages but also the channel aging effect.

### 4.2.3 Proposed Scheme with Cooperative PA

The schematic of the proposed scheme is illustrated in Fig. 4.2. Here, the objective is to avoid dynamic blockage and compensate for channel aging effect which, in return, will provide the high-speed vehicles with reliable high-rate connections.

With mobility, the availability of communication systems (possibly, using mmw-based narrow beamforming) faces different challenges including CSIT inaccuracy, beam misalignment and blockage. Particularly, with a blockage the path loss exponent increases from about 2.8 in the cases with LoS connections to almost 3.9 in NLoS communication, and outdated CSIT/out-of-beam signal reception leads to significant SINR drop and, consequently, service outage. Thus, it is desired to avoid dynamic blockage and acquire updated CSIT.

The key features of highway environments make it possible to solve the dynamic blockage/channel aging issues to some extent. In a highway, the vehicles are likely to drive along the same set of lanes with controlled speeds. Here, an example is the car-platooning setup, i.e., a set of vehicles traveling in a lane closely together with speed/direction controlled by the lead vehicle. Also, as shown in Fig. 4.2, in a highway, slow large vehicles (for instance, buses, trucks) travel typically in the outermost lanes, while the high-speed vehicles drive along the innermost lanes. Then, dynamic blockage occurs if a large vehicle drives between a user and its serving BS located, e.g., on lamp posts along the highway.

From a different perspective, as verified experimentally in, e.g., [20], [42], in a limited period such environments experience an essentially stationary electromagnetic standing wave pattern. Then, if the behind vehicle ends up in the same position as the front vehicle acquiring CSIT, it will experience the almost same radio environment, and the CSIT provided by the front vehicle can be used to improve the CSIT accuracy required for data transmission to the behind vehicle.

In this case, as we explain in the following, one can use blockage prediction and CSIT combination, and utilize cooperative communication/information exchange between the vehicles and BSs not only to avoid the channel aging effect but also the dynamic blockages. The details of such an innovative scheme are explained in the example below (see Fig. 4.2).

At Time Slot $T_1$:

- Being in Point A, the front vehicle, i.e., UE1 in Fig. 4.2, performs CSIT estimation and feeds back to BS1, using either TDD or FDD. Also, the front vehicle predicts a blockage by, e.g., a truck passing by. Here, the blockage can be predicted either before the UE1-BS1 link is blocked (using the sensors/cameras of UE1) or it can be detected in case a blockage has occurred and, as a result, a significant SINR drop is observed.

- Using cameras/sensors, UE1 finds the position and the speed of the blocker and the behind vehicle (UE2 in Fig. 4.2). Then, UE1 reports BS1 its own, the blocker's and the behind vehicle's position/speed information. Also, possibly, BS1 may be informed about the size of the vehicles.

- At BS1, receiving the vehicles speed/position information, BS1 determines $T_n$,

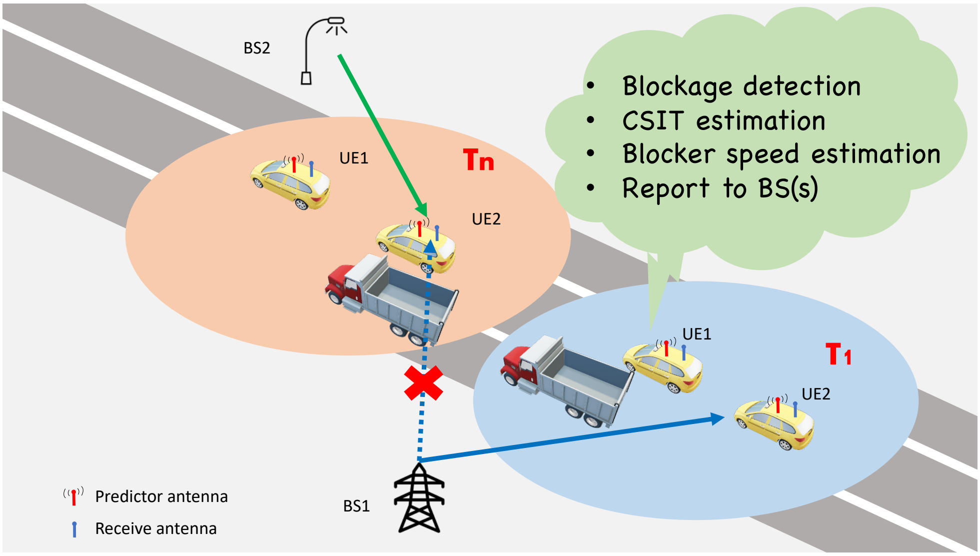


**Figure 4.2:** Illustration of the proposed large-scale cooperative PA (LSCPA) setup from Paper F [122].

i.e., the time slot in which the behind vehicles will be blocked by the blocker. Then, based on, e.g., the distance, QoS requirement, etc., BS1 decides if the data transmission in $T_n$ should be handovered to another BS (for instance, BS2 in Fig. 4.2), or still BS1 can serve the UE's successfully, e.g., by widening the beams, etc.

- If decided to handover, BS1 informs a secondary BS2 about the corresponding time slot $T_n$, as well as the vehicles speed/position information. Then, in $T_n$ BS2 serves the behind vehicle. The decision on handover depends on different parameters such as the QoS requirements, vehicles speed, blocker's size, etc. Also, different performance metrics can be considered for selecting the secondary BS (for instance, based on the distance, static blockages, etc.).

- At the same time, using the position/speed information, BS1 estimates the time slot in which UE2 will reach point A, i.e., the position in which we have the CSI from the BS1-UE1 communication. We denote this time slot by $T_m$ in the following.

At Time Slot $T_m$: If the data transmission is not handovered to BS2, BS1 performs CSIT acquisition from UE2 which is now at Point A. Then, BS1 combines the CSIT achieved from UE1 at $T_1$ and that obtained from UE2 at $T_m$ to improve the CSIT accuracy of Point A. Here, different methods can be considered to combine the acquired information. Then, using the combined CSIT, BS1 serves UE2 at $T_m$.

At Time Slot $T_n$: If handovered to BS2, BS2 performs typical CSIT acquisition of the BS2-UE2 link. With no handover, on the other hand, BS1 adapts its transmission parameters, e.g., beam width, to serve UE2.

In this way, blockage prediction avoids significant SINR drops. Also, the blockage prediction simplifies the handover process. This is because the BSs may have more than one slot gap for handover. This not only simplifies the scheduling, but also will reduce handover failure probability. Moreover, combining the CSIT acquired from different UE's compensates for channel aging, and improves the CSIT accuracy at given points. This gives the chance for high-rate/narrow beam data transmission. Finally, the proposed method simplifies the HARQ-based retransmissions and reduces the number of retransmissions/end-to-end (E2E) transmission delay. This is intuitively because when blockage is avoided, with high probability, large SNR drops are not experienced. Thus, even if a signal is not correctly decoded, it needs a small boost in the SNR which can be provided by, e.g., a single retransmission. Alternatively, one can rely only on diversity and use Type I HARQ with low implementation complexity. Thus, in summary, the proposed scheme enables the network to provide the vehicular UE's with fairly constant QoS. For detailed simulation results and discussions, see [122], i.e., the appended Paper F.

Here, the setup is presented for the simplest case with two vehicles. However, the setup can be applied in the cases with multiple vehicles in, e.g., a car platooning setup, where the benefit of the proposed scheme increases.

### 4.2.4 Dynamic Blockage Pre-Avoidance Using RIS

As we have shown in Paper G, the implementation of cooperative BSs can well avoid dynamic blockages. However, this may be not economically feasible to have multiple BSs in highways/rural areas. On the other hand, a large part of stationary blockages can be well avoided by network planning, which reduces the need for extra BSs in limited areas. Moreover, the implementation of cooperative BSs increases the energy consumption and the need for backhauling. For these reasons, it may be beneficial to use cheap solutions with no need for backhauling/handover, for which RIS is a good candidate. To enable multi-RIS communications, one needs to reduce the RIS selection and configuration overhead as well as the sensitivity to the vehicles speed. For this reason, we propose a large-scale based RIS pre-assignment (LSRPA) scheme in which the UE's and the blockers speed/position information is utilized along with the large-scale channel properties to predict and pre-select the RIS of interest, among multiple ones.

Consider the cases with either a macro or a small BS along a highway/intercity road, as illustrated in Fig. 4.3. With network planning, the BS location is normally optimized such that it covers a wide area of the road and static blockages are preferably avoided. However, dynamic blockages, due to, e.g., trucks, buses, are not encountered during the network planning and affect the achievable rate, specially

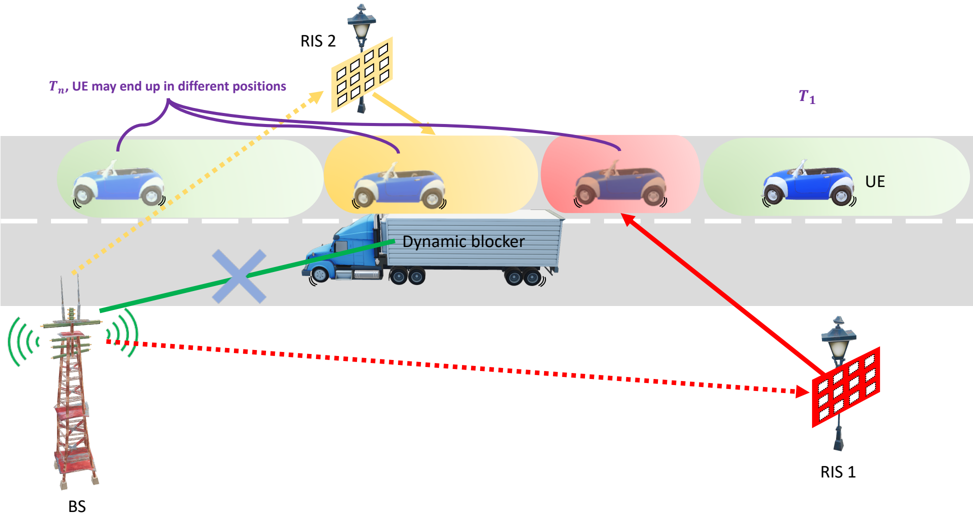


**Figure 4.3:** Illustration of the proposed LSRPA setup [Paper G].

in mmw bands. As a low-cost solution, to avoid dynamic blockages, $N$ RISs can be installed along the road which will provide back-up links to the vehicular UE's when required.

With such a setup, the main problem is to perform beam management in the BS and each RIS and select the best path. In the optimal case, one needs to know the instantaneous CSIT of all paths for joint beamforming optimization and RIS selection. This, however, not only increases the CSIT acquisition overhead, but also may not be feasible at moderate/high speeds due to the *channel aging* effect where the CSIT acquired at a position soon becomes outdated due to the UE high mobility.

With this background, the LSCPA scheme follows the following procedure:

At time slot $T_0$, if the vehicular UE detects a dynamic blockage, e.g., by a truck, it estimates the speed and the position of the blocker, e.g., using cameras, Lidars. Then, along with its own speed/position information, the UE informs the BS about the speed and position information of the dynamic blocker (As an alternative approach, each vehicle can inform the BS about its own speed/position information.). Knowing the blocker speed/position information at $T_0$, the BS predicts the blocker position at Slot $T_n$. Then, the BS utilizes the large-scale channel condition, i.e., the average performance which has been learned over time for the considered blocker position, to find the appropriate regions of interest to be covered by different RISs in different time slots. After that, the BS exploits the UE speed/position information provided at $T_0$ to predict the UE position at Slot $T_n$ and select the appropriate path towards the UE, either through direct BS-UE connection or via an RIS-assisted link. Finally, at Slot $T_n$, only the instantaneous CSIT of the pre-selected path, and not all possible paths, is acquired and the BS/RIS beamforming is adapted accordingly.

In this way, the LSCPA setup reduces the CSIT overhead/channel aging effect, and makes it possible to provide the vehicular UEs with fairly constant QoS. Note that, to apply the proposed scheme, one needs to have fairly accurate information about the UE/blocker speed and position information. However, this is achievable in, e.g., car platooning, connected vehicle or cruise control setups. Specially, in highways/inter-city roads, slow large vehicles (resp. high-speed vehicles) travel typically in the outermost (resp. innermost) lanes with predictable trajectory, which simplifies the positioning.

# CHAPTER 5

## Contributions and Future Work

This chapter summarizes the contributions of each appended publication and lays out possible directions for future work based on the topics in this thesis.

To have a clear view of the contributions and potential future directions of the thesis, Fig. 5.1 groups our work in different perspectives with a clear road map.

We start from the PA concept and develop analytical channel model with spatial mismatch in [100], i.e., appended Paper A, and propose a rate adaptation scheme to improve the system performance. Then, in [53], i.e., appended Paper B, we derive a semi-linear approximation of the Marcum-$Q$ function, which appears in the proposed PA channel model to simplify the analysis, where the effect of estimation error is also investigated. Then, in [114], [115], [123], i.e., appended Papers C-D and non-appended Paper I, we develop different resource allocation schemes in the PA system, namely, outage-limited power allocation, delay-limited average rate optimization, and rate adaptation with short packages, respectively. Above papers, i.e., Papers A-D, non-appended Paper I, consider single-input single-output (SISO) systems and focus on theoretical analysis from the information theory point of view.

Towards mmw MIMO system with data driven and simulation analysis, studies in [117], i.e., appended Paper E, provide an overview of the PA and MRs, and evaluate the performance of the PA system in both rural and urban area with BF. The work in Paper H review the latest developments of PA, and develop a velocity-aware transmission scheme in the PA setup. Focusing on blockage sensitivity at mmw band, a cooperative PA system under platooning setup in highways is proposed in [122], i.e., appended Paper F, while RIS is used in Paper G to perform the blockage pre-avoidance to reduce the CSIT acquisition overhead. Finally, low complexity

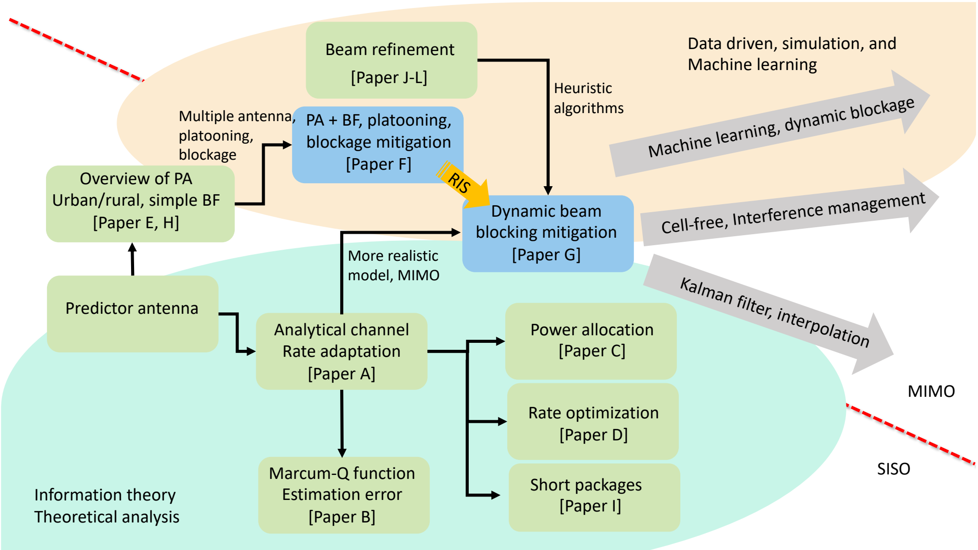


**Figure 5.1:** Illustration of the contributions and potential future directions of the thesis.

beam refinement algorithms are developed in [124], [125], and [126], which can be potentially applied in RIS beam optimizations.

The detailed contributions of appended/non-appended papers, as well as future directions, are presented below.

## 5.1 Paper A

**H. Guo, B. Makki, and T. Svensson, "Rate adaptation in predictor antenna systems," IEEE Wireless Communications Letters, vol. 9, no. 4, pp. 448-451, Apr. 2020.**

In this paper, we study the performance of PA systems in the presence of the spatial mismatch problem with rate adaptation. We derive closed-form expressions for the instantaneous throughput, the outage probability, and the throughput-optimized rate adaptation. Also, we take the temporal variation of the channel into account and evaluate the system performance in temporally-correlated conditions. The simulation and the analytical results show that, while PA-assisted adaptive rate adaptation leads to considerable performance improvement, the throughput and the outage probability are remarkably affected by the spatial mismatch and temporal correlations.

## 5.2 Paper B

**H. Guo, B. Makki, M.-S. Alouini, and T. Svensson, "A semi-linear approximation of the first-order Marcum $Q$-function with application to predictor antenna systems," IEEE Open Journal of Communication Society, vol. 2, pp. 273-286, Feb. 2021.**
In this paper, we first present a semi-linear approximation of the Marcum $Q$-function. Our proposed approximation is useful because it simplifies, e.g., various integral calculations including Marcum $Q$-function as well as various operations such as parameter optimization. Then, as an example of interest, we apply our proposed approximation approach to the performance analysis of PA systems. Considering spatial mismatch due to mobility, we derive closed-form expressions for the instantaneous and average throughput as well as the throughput-optimized rate allocation. As we show, our proposed approximation scheme enables us to analyze PA systems with high accuracy. Moreover, our results show that rate adaptation can improve the performance of PA systems with different levels of spatial mismatch.

## 5.3 Paper C

**H. Guo, B. Makki, M.-S. Alouini, and T. Svensson, "Power allocation in HARQ- based predictor antenna systems," IEEE Wireless Communication Letters, vol. 9, no. 12, pp. 2025-2029, Dec. 2020.**
In this work, we study the performance of PA systems using HARQ. Considering spatial mismatch due to the vehicle mobility, we derive closed-form expressions for the optimal power allocation and the minimum average power of the PA systems under different outage probability constraints. The results are presented for different types of HARQ protocols, and we study the effect of different parameters on the performance of PA systems. As we show, our proposed approximation scheme enables us to analyze PA systems with high accuracy. Moreover, for different vehicle speeds, we show that the HARQ-based feedback can reduce the outage-limited power consumption of PA systems by orders of magnitude.

## 5.4 Paper D

**H. Guo, B. Makki, M.-S. Alouini, and T. Svensson, "On the delay-limited average rate of HARQ-based predictor antenna systems," IEEE Wireless Communication Letters, vol. 10, no. 8, pp. 1628-1632, Aug. 2021.**
In this letter, we study the effect of spatial mismatch on the accuracy of channel state information estimation, and analyze the delay-constrained average rate of HARQ-based PA systems. We consider variable-INR HARQ protocol, and derive a closed-form expression for the maximum average rate subject to a maximum delay

constraint. Moreover, we study the effect of different parameters such as the vehicle speed, the antenna distance and the rate allocation on the system performance. The results indicate that, compared to the open-loop case, the delay-limited average rate is considerably improved with our proposed PA-HARQ scheme.

## 5.5 Paper E

**H. Guo, B. Makki, D.-T. Phan-Huy, E. Dahlman, M.-S. Alouini, T. Svensson, "Predictor antenna: A technique to boost the performance of moving relays," IEEE Communications Magazine, vol. 59, no. 7, pp. 80-86, Jul. 2021.**

In this article, we introduce the concept and the potential of PA systems. Moreover, summarizing the field trials for PAs and the 3GPP attempts on (moving) relays, we compare the performance of different PA and non-PA methods for vehicle communications in both urban and rural areas with the PA setup backhauled through terrestrial or satellite technology, respectively. As we show, with typical parameter settings and vehicle speeds, a single-antenna PA-assisted setup can boost the backhaul throughput of MRs, compared to state-of-the-art open-loop schemes, by up to 50 percent.

## 5.6 Paper F

**H. Guo, B. Makki, M.-S. Alouini, and T. Svensson, "High-rate uninterrupted internet-of-vehicle communications in highways: Dynamic blockage avoidance and CSIT acquisition," IEEE Communications Magazine, major revision, Jan. 2022.**

In future wireless networks, one of the use-cases of interest is IoV. Here, IoV refers to two different functionalities, namely, serving the in-vehicle users and supporting the connected-vehicle functionalities, where both can be well provided by the transceivers installed on top of vehicles. Such dual functionality of on-vehicle transceivers, however, implies strict rate and reliability requirements, for which one may need to utilize large bandwidths/BF, acquire up-to-date CSI and avoid blockages. In this article, we incorporate the recently proposed concept of PAs into the LSCPA setup where both temporal blockages and CSI out-dating are avoided via BSs/vehicles cooperation. Summarizing the ongoing standardization progress enabling IoV communications, we present the potentials and challenges of the LSCPA setup, and compare the effect of cooperative and non-cooperative schemes on the performance of IoV links. As we show, the BSs cooperation and blockage/CSI prediction can boost the performance of IoV links remarkably.

## 5.7 Paper G

**H. Guo, B. Makki, M. Åström, M.-S. Alouini, and T. Svensson, "Dynamic blockage pre-avoidance using reconfigurable intelligent surface," submitted to IEEE Communications Magazine, Jan. 2022.**

To avoid the blockage in IoV networks, different techniques have been proposed among which RIS is a candidate. RIS, however, has been mainly of interest in stationary/low mobility networks, due to its channel state information acquisition and beam management overhead as well as fuzzy reflection. In this article, we study the potentials and challenges of RIS-assisted dynamic blockage avoidance in high-speed IoV networks. Particularly, designing region-based RIS pre-selection as well as blockage prediction schemes, we show that RIS-assisted communication has the potential to boost the performance of IoV networks.

## 5.8 Related Contributions

Additional views on PA systems are provides in [123], [127], as complements for the included papers. In [123], we use the fundamental results on the achievable rate of finite block-length codes to study the system throughput and error probability in the presence of short packets. Particularly, we derive closed-form expressions for the error probability, the average transmit rate as well as the optimal rate allocation, and study the effect of different parameters on the performance of PA systems. The results indicate that rate adaptation under finite block-length codewords can improve the performance of the PA system with spatial mismatch.

Then, in [127], we review the PA concept and recent testbed- and theoretical- oriented studies on the PA. With promising progress on the PA studies, it has emerged as one promising enabler for MR and moving IAB nodes in next generation of mobile networks. Dealing with the speed/spatial mismatch problem, we propose a novel antenna selection scheme to fully utilize the velocity information and make the system more robust to speed variations. The simulation results further clarify the effect of spatial mismatch from different perspectives, and our proposed velocity-aware antenna selection scheme shows notable performance gains with multiple RA deployed at the vehicle side.

Another CSI-related application in vehicle communication is BF. As discussed in Chapter 1, the channel for vehicles changes rapidly, such that it is hard to acquire CSIT, especially during initial access. In [124], we study the performance of large-but-finite MIMO networks using codebook-based BF. Results show that the proposed genetic algorithm-based scheme can reach (almost) the same performance as in the exhaustive search-based scheme with considerably lower implementation complexity. Then, in [125], we extend our study in [124] to include BF at both the transmitter and the receiver side. Also, we compare different machine learning-based analog BF approaches for the beam refinement. As indicated in our results, our scheme outperforms the considered state-of-the-art schemes in terms of throughput. Moreover, when taking the user mobility into account, the proposed approach can remarkably reduce the algorithm running delay based on the beamforming results in the previous time slots. Finally, in [126], with collaborative users, we show that the end-to-end throughput can be improved by the data exchange through side links among users.

## 5.9 Future work

In this thesis, we have developed methods for uninterrupted high-rate communication at high speeds. Also, we proposed various schemes to, e.g., obtain accurate CSIT and avoid dynamic blockage, in order improve the system performance. Here are some potential directions for future work:

- Several results presented in the papers above rely on the assumption that the scattering environment around the RAs is isotropic and remains constant over the time period of interest in a small moving distance, although in [100] we briefly discuss about the system performance in temporally-correlated channels. To more accurately resemble reality, one could consider alternative models to evaluate the PA system, for example some mixture models with more time-varying properties [128].

- As a natural follow-up from above, one can consider more use cases for the PA system, such as satellite-train communication and vehicle localization, with different channel models and service requirements. Here, the results of [11], [30]–[38] can be supportive.

- Although in [117], [122] we numerically study the network performance in MIMO systems, to simplify the analysis/discussions, our works mainly consider SISO, i.e., with one antenna at the BS and one RA on the top of the vehicle at the receiver side. Though in [114], [115] we exploit PA as part of the data transmission, it is still interesting to see the full potential of deploying the PA system and when we should apply it over typical transceiver schemes. Deploying the PA in multiple antenna systems could be beneficial such as shown in the results of [21], [23], [129], it would be interesting to have more analytical analysis with PA-MIMO systems.

- As we discussed in Chapter 1, in PA systems we target at URLLC, i.e., delay/latency is crucial in the system design. Hence, there is a natural extension to perform finite blocklength analysis in the (HARQ-based) PA system. As opposed to the literature on finite blocklength studies, e.g., [106], [130], [131], here the channel in the retransmission round(s) is different from the one in the initial transmission due to mobility.

- Machine learning-based channel estimation/prediction has become powerful in various applications where the statistical model of channel does not exist or is not robust [132]–[134]. On the other hand, PA itself provides reliable feedback loop at the cost of additional resources. Using the PA setup to perform machine learning-based channel prediction would be a very valuable contribution.

# References


[1] Ericsson, "Ericsson mobility report," Jun. 2021.

[2] S. Dang, O. Amin, B. Shihada, and M.-S. Alouini, "What should 6G be?" *Nat. Electron.*, vol. 3, no. 1, pp. 20–29, Jan. 2020.

[3] J. G. Andrews, S. Buzzi, W. Choi, *et al.*, "What will 5G be?" *IEEE J. Sel. Areas Commun.*, vol. 32, pp. 1065–1082, Jun. 2014.

[4] A. Zaidi, F. Athley, J. Medbo, U. Gustavsson, G. Durisi, and X. Chen, *5G Physical Layer: Principles, Models and Technology Components*. Academic Press, 2018.

[5] M. Simsek, A. Aijaz, M. Dohler, J. Sachs, and G. Fettweis, "5G-enabled tactile internet," *IEEE J. Sel. Areas Commun.*, vol. 34, no. 3, pp. 460–473, Mar. 2016.

[6] A. Osseiran, F. Boccardi, V. Braun, *et al.*, "Scenarios for 5G mobile and wireless communications: The vision of the METIS project," *IEEE Commun. Mag.*, vol. 52, no. 5, pp. 26–35, May 2014.

[7] E. Dahlman, S. Parkvall, and J. Sköld, *5G NR: The Next Generation Wireless Access Technology*. Academic Press, 2018.

[8] C. Bockelmann, N. Pratas, H. Nikopour, *et al.*, "Massive machine-type communications in 5G: Physical and MAC-layer solutions," *IEEE Commun. Mag.*, vol. 54, no. 9, pp. 59–65, Sep. 2016.

[9] IMT-2020 (5G) Promotion Group, "5G Network Technology Architecture White Paper," May 2015, [Online]. Available: `http://www.imt-2020.org.cn/en`.

[10] Samsung Electronics Co. Ltd., "5G Vision," Feb. 2015, [Online]. Available: `https://www.samsung.com/global/business/networks/insights/5g/`.

[11] S. Yutao, J. Vihriala, A. Papadogiannis, M. Sternad, W. Yang, and T. Svensson, "Moving cells: A promising solution to boost performance for vehicular users," *IEEE Commun. Mag.*, vol. 51, no. 6, pp. 62–68, Jun. 2013.

[12] F. Harrysson, J. Medbo, T. Hult, and F. Tufvesson, "Experimental investigation of the directional outdoor-to-in-car propagation channel," *IEEE Trans. Veh. Technol.*, vol. 62, no. 6, pp. 2532–2543, Jul. 2013.

[13] O. Teyeb, A. Muhammad, G. Mildh, E. Dahlman, F. Barac, and B. Makki, "Integrated access backhauled networks," in *Proc. IEEE VTC Fall*, Honolulu, HI, USA, Sep. 2019, pp. 1–5.

[14] C. Madapatha, B. Makki, C. Fang, *et al.*, "On integrated access and backhaul networks: Current status and potentials," *IEEE Open J. Commun. Soc.*, vol. 1, pp. 1374–1389, Dec. 2020.

[15] C. Madapatha, B. Makki, A. Muhammad, E. Dahlman, M.-S. Alouini, and T. Svensson, "On Topology Optimization and Routing in Integrated Access and Backhaul Networks: A Genetic Algorithm-Based Approach," *IEEE Open J. Commun. Soc.*, vol. 2, pp. 2273–2291, Sep. 2021.

[16] Document 3GPP TR 36.913, "Requirements for Further Advancements for Evolved Universal Terrestrial Radio Access (EUTRA) (LTE-Advanced)," Sep. 2014, [Online]. Available: `https://portal.3gpp.org`.

[17] J. Wu and P. Fan, "A survey on high mobility wireless communications: Challenges, opportunities and solutions," *IEEE Access*, vol. 4, pp. 450–476, Jan. 2016.

[18] S. Rezvani, N. M. Yamchi, M. R. Javan, and E. A. Jorswieck, "Resource allocation in virtualized CoMP-NOMA HetNets: Multi-connectivity for joint transmission," *IEEE Trans. Commun.*, vol. 69, no. 6, pp. 4172–4185, Jun. 2021.

[19] M. Sternad, M. Grieger, R. Apelfröjd, T. Svensson, D. Aronsson, and A. B. Martinez, "Using predictor antennas for long-range prediction of fast fading for moving relays," in *Proc. IEEE WCNCW*, Paris, France, Apr. 2012, pp. 253–257.

[20] J. Björsell, M. Sternad, and M. Grieger, "Using predictor antennas for the prediction of small-scale fading provides an order-of-magnitude improvement of prediction horizons," in *Proc. IEEE ICCW*, Paris, France, May 2017, pp. 54–60.

[21] D.-T. Phan-Huy, S. Wesemann, J. Björsell, and M. Sternad, "Adaptive massive MIMO for fast moving connected vehicles: It will work with predictor antennas!" In *Proc. IEEE WSA*, Bochum, Germany, Mar. 2018, pp. 1–8.

[22] R. Apelfröjd, J. Björsell, M. Sternad, and D. Phan-Huy, "Kalman smoothing for irregular pilot patterns; a case study for predictor antennas in TDD systems," in *Proc. IEEE PIMRC*, Bologna, Italy, Sep. 2018, pp. 1–7.

[23] D.-T. Phan-Huy, M. Sternad, and T. Svensson, “Making 5G adaptive antennas work for very fast moving vehicles,” *IEEE Intell. Transp. Syst. Mag.*, vol. 7, no. 2, pp. 71–84, Apr. 2015.

[24] N. Jamaly, T. Svensson, and A. Derneryd, “Effects of coupling and overspeeding on performance of predictor antenna systems in wireless moving relays,” *IET Microw., Antennas Propag.*, vol. 13, no. 3, pp. 367–372, Feb. 2019.

[25] Q. Wu and R. Zhang, “Towards smart and reconfigurable environment: Intelligent reflecting surface aided wireless network,” *IEEE Commun. Mag.*, vol. 58, no. 1, pp. 106–112, Jan. 2020.

[26] A. Khalili, E. M. Monfared, S. Zargari, M. R. Javan, N. Mokari, and E. A. Jorswieck, “Resource management for transmit power minimization in UAV-assisted RIS HetNets supported by dual connectivity,” *IEEE Trans. Wireless Commun.*, pp. 1–1, 2021.

[27] B. Di, H. Zhang, L. Song, Y. Li, Z. Han, and H. V. Poor, “Hybrid beamforming for reconfigurable intelligent surface based multi-user communications: Achievable rates with limited discrete phase shifts,” *IEEE J. Sel. Areas Commun.*, vol. 38, no. 8, pp. 1809–1822, Aug. 2020.

[28] M. Gao, B. Ai, Y. Niu, Z. Han, and Z. Zhong, “IRS-assisted high-speed train communications: Outage probability minimization with statistical CSI,” in *Proc. IEEE ICC*, Montreal, QC, Canada, Jun. 2021, pp. 1–6.

[29] M. Z. Bocus, C. P. Dettmann, and J. P. Coon, “An approximation of the first order Marcum $Q$-function with application to network connectivity analysis,” *IEEE Commun. Lett.*, vol. 17, no. 3, pp. 499–502, Mar. 2013.

[30] T. Shim, J. Park, S. Ko, S. Kim, B. Lee, and J. Choi, “Traffic convexity aware cellular networks: a vehicular heavy user perspective,” *IEEE Wireless Commun.*, vol. 23, no. 1, pp. 88–94, Feb. 2016.

[31] B. Lannoo, D. Colle, M. Pickavet, and P. Demeester, “Radio-over-fiber-based solution to provide broadband internet access to train passengers,” *IEEE Commun. Mag.*, vol. 45, no. 2, pp. 56–62, Feb. 2007.

[32] J. Wang, H. Zhu, and N. J. Gomes, “Distributed antenna systems for mobile communications in high speed trains,” *IEEE J. Sel. Areas Commun.*, vol. 30, no. 4, pp. 675–683, Apr. 2012.

[33] P. T. Dat, A. Kanno, N. Yamamoto, and T. Kawanishi, “WDM RoF-MMW and linearly located distributed antenna system for future high-speed railway communications,” *IEEE Commun. Mag.*, vol. 53, no. 10, pp. 86–94, Oct. 2015.

[34] A. O. Laiyemo, H. Pennanen, P. Pirinen, and M. Latva-Aho, “Transmission strategies for throughput maximization in high-speed-train communications: From theoretical study to practical algorithms,” *IEEE Trans. Veh. Technol.*, vol. 66, no. 4, pp. 2997–3011, Apr. 2017.

[35] A. S. W. Marzuki, I. Ahmad, D. Habibi, and Q. V. Phung, "Mobile small cells: Broadband access solution for public transport users," *IEEE Commun. Mag.*, vol. 55, no. 6, pp. 190–197, Jun. 2017.

[36] S. Andreev, V. Petrov, M. Dohler, and H. Yanikomeroglu, "Future of ultra-dense networks beyond 5G: Harnessing heterogeneous moving cells," *IEEE Commun. Mag.*, vol. 57, no. 6, pp. 66–92, Jun. 2019.

[37] F. Haider, C. X. Wang, B. Ai, H. Haas, and E. Hepsaydir, "Spectral/Energy efficiency tradeoff of cellular systems with mobile femtocell deployment," *IEEE Trans. Veh. Technol.*, vol. 65, no. 5, pp. 3389–3400, May 2016.

[38] M. Patra, R. Thakur, and C. S. R. Murthy, "Improving delay and energy efficiency of vehicular networks using mobile femto access points," *IEEE Trans. Veh. Technol.*, vol. 66, no. 2, pp. 1496–1505, Feb. 2017.

[39] D. Aronsson, "Channel estimation and prediction for MIMO OFDM systems - Key design and Performance Aspects of Kalman-based Algorithms," Ph.D. dissertation, Uppsala University, Uppsala, Sweden, Mar. 2011.

[40] T. Ekman, "Predictions of mobile radio channels," Ph.D. dissertation, Uppsala University, Uppsala, Sweden, Oct. 2002.

[41] W. Zirwas and M. Haardt, "Channel prediction for B4G radio systems," in *Proc. IEEE VTC Spring*, Dresden, Germany, Jun. 2013.

[42] J. Björsell, M. Sternad, and M. Grieger, "Predictor antennas in action," in *Proc. IEEE PIMRC*, Montreal, Quebec, Canada, Oct. 2017, pp. 1–7.

[43] N. Jamaly, R. Apelfröjd, A. Belen Martinez, *et al.*, "Analysis and measurement of multiple antenna systems for fading channel prediction in moving relays," in *Proc. IEEE EuCAP*, The Hague, The Netherlands, Apr. 2014, pp. 2015–2019.

[44] F. Vatalaro, "Generalized Rice-lognormal channel model for wireless communications," *Electron. Lett.*, vol. 31, pp. 1899–1900, Oct. 1995.

[45] T. T. Tjhung and C. C. Chai, "Fade statistics in Nakagami-lognormal channels," *IEEE Trans. Commun.*, vol. 47, pp. 1769–1772, Dec. 1999.

[46] J. Tsao, D. Porrat, and D. Tse, "Prediction and modeling for the time-evolving ultra-wideband channel," *IEEE J. Sel. Topics Signal Process.*, vol. 1, no. 3, pp. 340–356, Oct. 2007.

[47] B. Makki and T. Eriksson, "Feedback subsampling in temporally-correlated slowly-fading channels using quantized CSI," *IEEE Trans. Commun.*, vol. 61, no. 6, pp. 2282–2294, Jun. 2013.

[48] B. Makki, T. Svensson, and M. Debbah, "Reinforcement-based data transmission in temporally-correlated fading channels: Partial CSIT scenario," in *Proc. IEEE ISWCS*, Barcelona, Spain, Aug. 2014, pp. 176–181.

[49] J. Jose, A. Ashikhmin, T. L. Marzetta, and S. Vishwanath, "Pilot contamination and precoding in Multi-Cell TDD systems," *IEEE Trans. Wireless Commun.*, vol. 10, no. 8, pp. 2640–2651, Jun. 2011.

[50] D. Mi, M. Dianati, L. Zhang, S. Muhaidat, and R. Tafazolli, "Massive MIMO performance with imperfect channel reciprocity and channel estimation error," *IEEE Trans. Commun.*, vol. 65, no. 9, pp. 3734–3749, Sep. 2017.

[51] L. Lu, G. Y. Li, A. L. Swindlehurst, A. Ashikhmin, and R. Zhang, "An overview of massive MIMO: Benefits and challenges," *IEEE J. Sel. Topics Signal Process.*, vol. 8, no. 5, pp. 742–758, Oct. 2014.

[52] A. Tolli, M. Codreanu, and M. Juntti, "Compensation of non-reciprocal interference in adaptive MIMO-OFDM cellular systems," *IEEE Trans. Wireless Commun.*, vol. 6, no. 2, pp. 545–555, Feb. 2017.

[53] H. Guo, B. Makki, M.-S. Alouini, and T. Svensson, "A semi-linear approximation of the first-order Marcum $Q$-function with application to predictor antenna systems," *IEEE Open J. Commun. Soc.*, vol. 2, pp. 273–286, Feb. 2021.

[54] H. Shin and J. H. Lee, "Capacity of multiple-antenna fading channels: Spatial fading correlation, double scattering, and keyhole," *IEEE Trans. Inf. Theory*, vol. 49, no. 10, pp. 2636–2647, Oct. 2003.

[55] E. Jorswieck and H. Boche, "Channel capacity and capacity-range of beamforming in MIMO wireless systems under correlated fading with covariance feedback," *IEEE Trans. Wireless Commun.*, vol. 3, no. 5, pp. 1543–1553, Sep. 2004.

[56] D. Chizhik, F. Rashid-Farrokhi, J. Ling, and A. Lozano, "Effect of antenna separation on the capacity of BLAST in correlated channels," *IEEE Commun. Lett.*, vol. 4, no. 11, pp. 337–339, Nov. 2000.

[57] M. S. Abramowitz and I. Stegun, "Handbook of Mathematical Functions with Formulas, Graphs, and Mathematical Tables," *New York: Dover*, 1972.

[58] C. Wang, E. K. S. Au, R. D. Murch, W. H. Mow, R. S. Cheng, and V. Lau, "On the performance of the MIMO zero-forcing receiver in the presence of channel estimation error," *IEEE Trans. Wireless Commun.*, vol. 6, no. 3, pp. 805–810, Mar. 2007.

[59] C. W. Helstrom, *Elements of Signal Detection and Estimation.* Prentice-Hall, Inc., 1994.

[60] B. Makki and T. Eriksson, "On the capacity of Rayleigh-fading correlated spectrum sharing networks," *Eurasip J. Wireless Commun. Netw.*, vol. 2011, no. 1, p. 83, Aug. 2011.

[61] B. Makki, T. Svensson, K. Buisman, J. Perez, and M.-S. Alouini, "Wireless energy and information transmission in FSO and RF-FSO links," *IEEE Wireless Commun. Lett.*, vol. 7, no. 1, pp. 90–93, Feb. 2018.

[62] B. Makki, T. Eriksson, and T. Svensson, "On the performance of the relay ARQ networks," *IEEE Trans. Veh. Technol.*, vol. 65, no. 4, pp. 2078–2096, Apr. 2016.

[63] M. K. Simon and M.-S. Alouini, "Some new results for integrals involving the generalized Marcum $Q$ function and their application to performance evaluation over fading channels," *IEEE Trans. Wireless Commun.*, vol. 2, no. 4, pp. 611–615, Jul. 2003.

[64] H. A. Suraweera, P. J. Smith, and M. Shafi, "Capacity limits and performance analysis of cognitive radio with imperfect channel knowledge," *IEEE Trans. Veh. Technol.*, vol. 59, no. 4, pp. 1811–1822, May 2010.

[65] M. Kang and M.-S. Alouini, "Largest eigenvalue of complex Wishart matrices and performance analysis of MIMO MRC systems," *IEEE J. Sel. Areas Commun.*, vol. 21, no. 3, pp. 418–426, Apr. 2003.

[66] Y. Chen and C. Tellambura, "Distribution functions of selection combiner output in equally correlated Rayleigh, Rician, and Nakagami-$m$ fading channels," *IEEE Trans. Commun.*, vol. 52, no. 11, pp. 1948–1956, Nov. 2004.

[67] Y. Ma and C. Choy Chai, "Unified error probability analysis for generalized selection combining in Nakagami fading channels," *IEEE J. Sel. Areas Commun.*, vol. 18, no. 11, pp. 2198–2210, Nov. 2000.

[68] Q. T. Zhang and H. G. Lu, "A general analytical approach to multi-branch selection combining over various spatially correlated fading channels," *IEEE Trans. Commun.*, vol. 50, no. 7, pp. 1066–1073, Jul. 2002.

[69] A. Ghasemi and E. S. Sousa, "Spectrum sensing in cognitive radio networks: Requirements, challenges and design trade-offs," *IEEE Commun. Mag.*, vol. 46, no. 4, pp. 32–39, Apr. 2008.

[70] F. F. Digham, M.-S. Alouini, and M. K. Simon, "On the energy detection of unknown signals over fading channels," *IEEE Trans. Commun.*, vol. 55, no. 1, pp. 21–24, Jan. 2007.

[71] M. K. Simon and M.-S. Alouini, "Digital communication over generalized fading channels: A unified approach to performance analysis," *Wiley, New York*, 2005.

[72] K. Cao and X. Gao, "Solutions to generalized integrals involving the generalized Marcum $Q$-function with application to energy detection," *IEEE Commun. Lett.*, vol. 20, no. 9, pp. 1780–1783, Sep. 2016.

[73] P. C. Sofotasios, S. Muhaidat, G. K. Karagiannidis, and B. S. Sharif, "Solutions to integrals involving the Marcum $Q$-function and applications," *IEEE Signal Process. Lett.*, vol. 22, no. 10, pp. 1752–1756, Oct. 2015.

[74] G. Cui, L. Kong, X. Yang, and D. Ran, "Two useful integrals involving generalised Marcum $Q$-function," *Electron. Lett.*, vol. 48, no. 16, pp. 1017–1018, Aug. 2012.

[75] M. M. Azari, F. Rosas, K. Chen, and S. Pollin, "Ultra reliable UAV communication using altitude and cooperation diversity," *IEEE Trans. Commun.*, vol. 66, no. 1, pp. 330–344, Jan. 2018.

[76] M. M. Alam, S. Bhattarai, L. Hong, and S. Shetty, "Robust transmit beamforming against steering vector uncertainty in cognitive radio networks," in *Proc. IEEE INFOCOMW*, Toronto, Canada, Apr. 2014, pp. 700–705.

[77] B. Gao, M. Lin, K. An, G. Zheng, L. Zhao, and X. Liu, "ADMM-based optimal power control for cognitive satellite terrestrial uplink networks," *IEEE Access*, vol. 6, pp. 64 757–64 765, Oct. 2018.

[78] H. Shen, W. Xu, and C. Zhao, "Outage minimized full-duplex multiantenna DF relaying with CSI uncertainty," *IEEE Trans. Veh. Technol.*, vol. 67, no. 9, pp. 9000–9005, Sep. 2018.

[79] T. Song, Q. Wang, M. Wu, T. Ohtsuki, M. Gurusamy, and P. Kam, "Impact of pointing errors on the error performance of intersatellite laser communications," *J. Lightw. Technol.*, vol. 35, no. 14, pp. 3082–3091, Jul. 2017.

[80] H. Tang, L. Chai, and X. Wan, "An augmented generalized likelihood ratio test detector for signal detection in clutter and noise," *IEEE Access*, vol. 7, pp. 163 478–163 486, Nov. 2019.

[81] N. Y. Ermolova and O. Tirkkonen, "Laplace transform of product of generalized Marcum Q, Bessel I, and power functions with applications," *IEEE Trans. Signal Process.*, vol. 62, no. 11, pp. 2938–2944, Apr. 2014.

[82] K. P. Peppas, G. C. Alexandropoulos, and P. T. Mathiopoulos, "Performance analysis of dual-hop AF relaying systems over mixed $\eta-\mu$ and $\kappa-\mu$ fading channels," *IEEE Trans. Veh. Technol.*, vol. 62, no. 7, pp. 3149–3163, Mar. 2013.

[83] D. Morales-Jimenez, F. J. Lopez-Martinez, E. Martos-Naya, J. F. Paris, and A. Lozano, "Connections between the generalized Marcum $Q$-function and a class of Hypergeometric functions," *IEEE Trans. Inf. Theory*, vol. 60, no. 2, pp. 1077–1082, Nov. 2014.

[84] H. Fu and P. Kam, "Exponential-type bounds on the first-order Marcum $Q$-function," in *Proc. IEEE GLOBECOM*, Houston, Texas, USA, Dec. 2011, pp. 1–5.

[85] X. Zhao, D. Gong, and Y. Li, "Tight geometric bound for Marcum $Q$-function," *Electron. Lett.*, vol. 44, no. 5, pp. 340–341, Feb. 2008.

[86] M. K. Simon and M.-S. Alouini, "Exponential-type bounds on the generalized Marcum $Q$-function with application to error probability analysis over fading channels," *IEEE Trans. Commun.*, vol. 48, no. 3, pp. 359–366, Mar. 2000.

[87] A. Annamalai and C. Tellambura, "Cauchy–Schwarz bound on the generalized Marcum $Q$-function with applications," *Wireless Commun. Mob. Comput.*, vol. 1, no. 2, pp. 243–253, Apr. 2001.

[88] P. C. Sofotasios and S. Freear, "Novel expressions for the Marcum and one dimensional $Q$-functions," in *Proc. IEEE ISWCS*, York, United Kingdom, Sep. 2010, pp. 736–740.

[89] R. Li, P. Y. Kam, and H. Fu, "New representations and bounds for the generalized Marcum $Q$-function via a geometric approach, and an application," *IEEE Trans. Commun.*, vol. 58, no. 1, pp. 157–169, Jan. 2010.

[90] S. András, A. Baricz, and Y. Sun, "The generalized Marcum Q-function: an orthogonal polynomial approach," *Acta Universitatis Sapientiae Mathematica*, vol. 3, no. 1, pp. 60–76, Oct. 2011.

[91] S. Gaur and A. Annamalai, "Some integrals involving the $Q_m(a\sqrt{x}, b\sqrt{x})$ with application to error probability analysis of diversity receivers," *IEEE Trans. Veh. Technol.*, vol. 52, no. 6, pp. 1568–1575, Nov. 2003.

[92] P. Y. Kam and R. Li, "Computing and bounding the first-order Marcum $Q$-function: a geometric approach," *IEEE Trans. Commun.*, vol. 56, no. 7, pp. 1101–1110, Jul. 2008.

[93] G. E. Corazza and G. Ferrari, "New bounds for the Marcum $Q$-function," *IEEE Trans. Inf. Theory*, vol. 48, no. 11, pp. 3003–3008, Nov. 2002.

[94] Á. Baricz and Y. Sun, "New bounds for the generalized Marcum $Q$-function," *IEEE Trans. Inf. Theory*, vol. 55, no. 7, pp. 3091–3100, Jul. 2009.

[95] M. Chiani, "Integral representation and bounds for Marcum $Q$-function," *Electron. Lett.*, vol. 35, no. 6, pp. 445–446, Mar. 1999.

[96] P. C. Sofotasios, T. A. Tsiftsis, Y. A. Brychkov, S. Freear, M. Valkama, and G. K. Karagiannidis, "Analytic expressions and bounds for special functions and applications in communication theory," *IEEE Trans. Inf. Theory*, vol. 60, no. 12, pp. 7798–7823, Dec. 2014.

[97] E. Biglieri, J. Proakis, and S. Shamai, "Fading channels: Information-theoretic and communications aspects," *IEEE Trans. Inf. Theory*, vol. 44, no. 6, pp. 2619–2692, Oct. 1998.

[98] S. Verdú and Te Sun Han, "A general formula for channel capacity," *IEEE Trans. Inf. Theory*, vol. 40, no. 4, pp. 1147–1157, Jul. 1994.

[99] B. Makki and T. Eriksson, "On the performance of MIMO-ARQ systems with channel state information at the receiver," *IEEE Trans. Commun.*, vol. 62, no. 5, pp. 1588–1603, May 2014.

[100] H. Guo, B. Makki, and T. Svensson, "Rate adaptation in predictor antenna systems," *IEEE Wireless Commun. Lett.*, vol. 9, no. 4, pp. 448–451, Apr. 2020.

[101] G. Caire and D. Tuninetti, "The throughput of hybrid-ARQ protocols for the Gaussian collision channel," *IEEE Trans. Inf. Theory*, vol. 47, no. 5, pp. 1971–1988, Jul. 2001.

[102] B. Makki and T. Eriksson, "On hybrid ARQ and quantized CSI feedback schemes in quasi-static fading channels," *IEEE Trans. Commun.*, vol. 60, no. 4, pp. 986–997, Apr. 2012.

[103] G. Caire, G. Taricco, and E. Biglieri, "Optimum power control over fading channels," *IEEE Trans. Inf. Theory*, vol. 45, no. 5, pp. 1468–1489, Jul. 1999.

[104] S. Lee, W. Su, S. Batalama, and J. D. Matyjas, "Cooperative decode-and-forward ARQ relaying: Performance analysis and power optimization," *IEEE Trans. Wireless Commun.*, vol. 9, no. 8, pp. 2632–2642, Aug. 2010.

[105] B. Makki, A. Graell i Amat, and T. Eriksson, "Green communication via power-optimized HARQ protocols," *IEEE Trans. Veh. Technol.*, vol. 63, no. 1, pp. 161–177, Jan. 2014.

[106] B. Makki, T. Svensson, and M. Zorzi, "Green communication via Type-I ARQ: Finite block-length analysis," in *Proc. IEEE GLOBECOM*, Austin, TX, USA, Dec. 2014, pp. 2673–2677.

[107] P. Wu and N. Jindal, "Performance of hybrid-ARQ in block-fading channels: A fixed outage probability analysis," *IEEE Trans. Commun.*, vol. 58, no. 4, pp. 1129–1141, Apr. 2010.

[108] W. Su, S. Lee, D. A. Pados, and J. D. Matyjas, "Optimal power assignment for minimizing the average total transmission power in hybrid-ARQ Rayleigh fading links," *IEEE Trans. Commun.*, vol. 59, no. 7, pp. 1867–1877, Jul. 2011.

[109] T. V. K. Chaitanya and E. G. Larsson, "Outage-optimal power allocation for hybrid ARQ with incremental redundancy," *IEEE Trans. Wireless Commun.*, vol. 10, no. 7, pp. 2069–2074, Jul. 2011.

[110] H. Seo and B. G. Lee, "Optimal transmission power for single- and multi-hop links in wireless packet networks with ARQ capability," *IEEE Trans. Commun.*, vol. 55, no. 5, pp. 996–1006, May 2007.

[111] D. V. Djonin, A. K. Karmokar, and V. K. Bhargava, "Joint rate and power adaptation for type-I hybrid ARQ systems over correlated fading channels under different buffer-cost constraints," *IEEE Trans. Veh. Technol.*, vol. 57, no. 1, pp. 421–435, Jan. 2008.

[112] B. Makki, A. Graell i Amat, and T. Eriksson, "On ARQ-based fast-fading channels," *IEEE Commun. Lett.*, vol. 16, no. 12, pp. 1921–1924, Dec. 2012.

[113] A. Chelli, E. Zedini, M.-S. Alouini, J. R. Barry, and M. Pätzold, "Performance and delay analysis of hybrid ARQ with incremental redundancy over double Rayleigh fading channels," *IEEE Trans. Wireless Commun.*, vol. 13, no. 11, pp. 6245–6258, Nov. 2014.

[114] H. Guo, B. Makki, M.-S. Alouini, and T. Svensson, "On delay-limited average rate of HARQ-based predictor antenna systems," *IEEE Wireless Commun. Lett.*, vol. 10, no. 8, pp. 1628–1632, Aug. 2021.

[115] ——, "Power allocation in HARQ-based predictor antenna systems," *IEEE Wireless Commun. Lett.*, vol. 9, no. 12, pp. 2025–2029, Dec. 2020.

[116] B. Makki, T. Svensson, T. Eriksson, and M.-S. Alouini, "On the performance of RF-FSO links with and without hybrid ARQ," *IEEE Trans. Wireless Commun.*, vol. 15, no. 7, pp. 4928–4943, Jul. 2016.

[117] H. Guo, B. Makki, D.-T. Phan-Huy, E. Dahlman, M.-S. Alouini, and T. Svensson, "Predictor antenna: A technique to boost the performance of moving relays," *IEEE Commun. Mag.*, vol. 59, no. 7, pp. 80–86, Jul. 2021.

[118] D. T. Phan-Huy, M. Sternad, T. Svensson, *et al.*, "5G on board: How many antennas do we need on connected cars?" In *Proc. IEEE Globecom Workshops*, Washington, DC, USA, Dec. 2016.

[119] G. B. A. Grassi G. Piro and D. Phan-Huy, "A system level evaluation of SRTA-PI transmission scheme in the high-speed train use case," in *25th International Conference on Telecommunications (ICT)*, St. Malo, Jan. 2018, pp. 165–169.

[120] D. Yang, L.-L. Yang, and L. Hanzo, "DFT-based beamforming weight-vector codebook design for spatially correlated channels in the unitary precoding aided multiuser downlink," in *Proc. IEEE ICC*, Cape Town, South Africa, May 2010, pp. 1–5.

[121] S. Khosravi, H. Shokri-Ghadikolaei, and M. Petrova, "Learning-based handover in mobile millimeter-wave networks," *IEEE Trans. Cogn. Commun. Netw.*, vol. 7, no. 2, pp. 663–674, Jun. 2021.

[122] H. Guo, B. Makki, M.-S. Alouini, and T. Svensson, "High-rate uninterrupted Internet-of-vehicle communications in highways: Dynamic blockage avoidance and CSIT acquisition," Sep. 2021, [Online]. Available: `https://arxiv.org/abs/2109.12878`.

[123] H. Guo, B. Makki, and T. Svensson, "Predictor antennas for moving relays: Finite block-length analysis," in *2020 3rd International Conference on Advanced Communication Technologies and Networking (CommNet)*, Marrakech, Morocco, Sep. 2020, pp. 1–8.

[124] H. Guo, B. Makki, and T. Svensson, "A genetic algorithm-based beamforming approach for delay-constrained networks," in *Proc. IEEE WiOpt*, Paris, France, May 2017, pp. 1–7.

[125] ——, "A comparison of beam refinement algorithms for millimeter wave initial access," in *Proc. IEEE PIMRC*, Montreal, QC, Canada, Oct. 2017, pp. 1–7.

[126] ——, "Genetic algorithm-based beam refinement for initial access in millimeter wave mobile networks," *Wireless Commun. Mob. Comput.*, vol. 2018, Jun. 2018.

[127] H. Guo, B. Makki, and T. Svensson, "Velocity-aware antenna selection in predictor antenna systems," Sep. 2021, [Online]. Available: `https://arxiv.org/abs/2110.00064`.

[128] A. Abdi, W. C. Lau, M.-S. Alouini, and M. Kaveh, "A new simple model for land mobile satellite channels: First- and second-order statistics," *IEEE Trans. on Wireless Commun.*, vol. 2, no. 3, pp. 519–528, May 2003.

[129] D. T. Phan-Huy, M. Sternad, and T. Svensson, "Adaptive large MISO downlink with predictor antenna array for very fast moving vehicles," in *Proc. IEEE ICCVE*, Las Vegas, Nevada, USA, Dec. 2013, pp. 331–336.

[130] B. Makki, T. Svensson, and M. Zorzi, "Finite block-length analysis of the incremental redundancy HARQ," *IEEE Wireless. Commun. Lett.*, vol. 3, no. 5, pp. 529–532, Oct. 2014.

[131] W. Yang, G. Durisi, T. Koch, and Y. Polyanskiy, "Quasi-static multiple-antenna fading channels at finite blocklength," *IEEE Trans. Inf. Theory*, vol. 60, no. 7, Jul. 2014.

[132] H. Ye, G. Y. Li, and B. Juang, "Power of deep learning for channel estimation and signal detection in OFDM systems," *IEEE Wireless Commun. Lett.*, vol. 7, no. 1, pp. 114–117, Sep. 2018.

[133] C. Wen, W. Shih, and S. Jin, "Deep learning for massive MIMO CSI feedback," *IEEE Wireless Commun. Lett.*, vol. 7, no. 5, pp. 748–751, Mar. 2018.

[134] K. Feng, Q. Wang, X. Li, and C. Wen, "Deep reinforcement learning based intelligent reflecting surface optimization for MISO communication systems," *IEEE Wireless Commun. Lett.*, pp. 745–749, Jan. 2020.

# Part II

# Papers